

새로운 나노 광전자공학 – 플라즈모닉스

이 병호

서울대학교 전기공학부

byoungho@snu.ac.kr



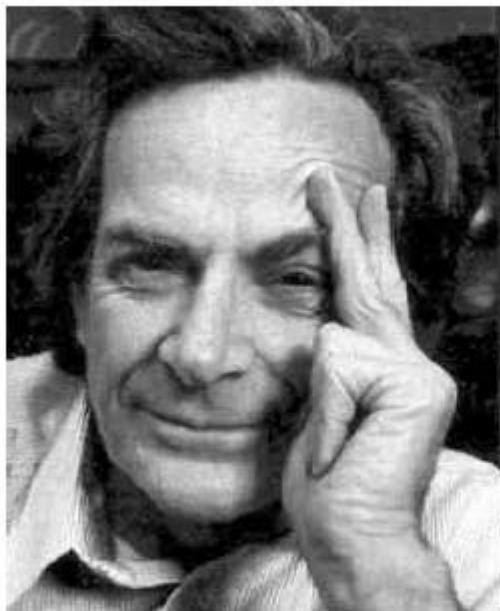
Seoul National University



Contents

- Introduction
- Photonic crystals
- Vectorial diffractive optics
- Plasmonics - Surface plasmon polaritons
- Concluding remarks





"There is Plenty of Room at the Bottom"

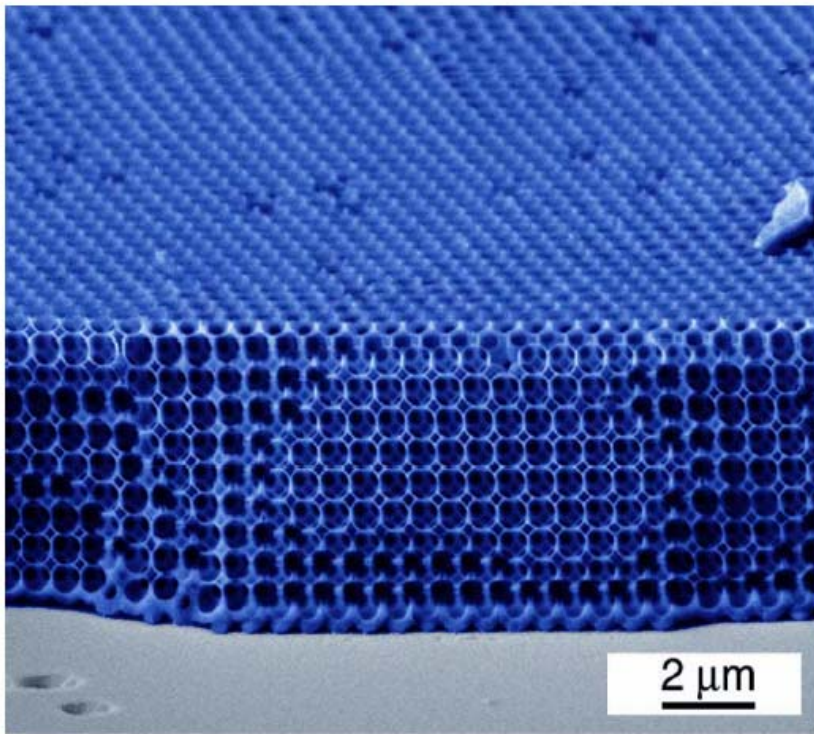
Prof. Richard P. Feynman

December, 1959

California Institute of Technology

<http://www.zyvex.com/nanotech/feynman.html>

Photonic crystals



[Y. A. Vlasov *et al.*, *Nature* **414**, 289 (2001).]

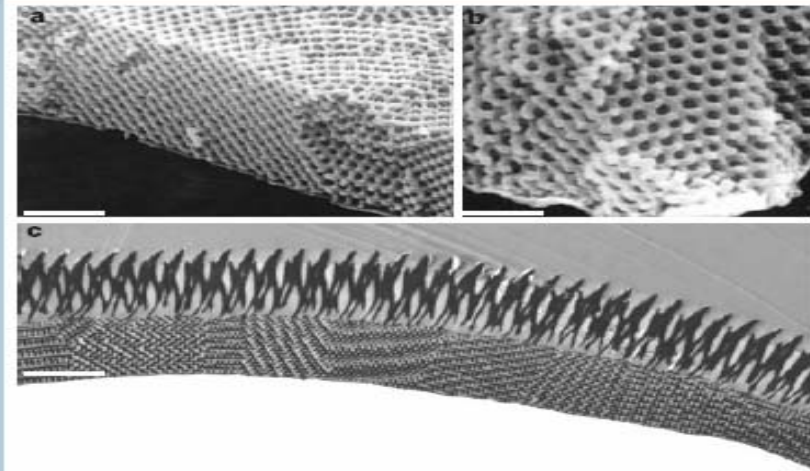


Figure 6 The green colour of *Papilio sesostris* is created by a photonic crystal. a, b,

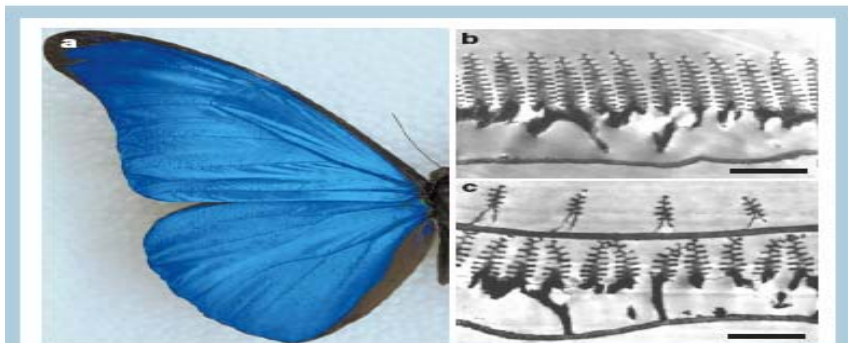
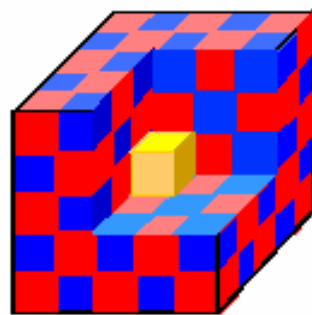
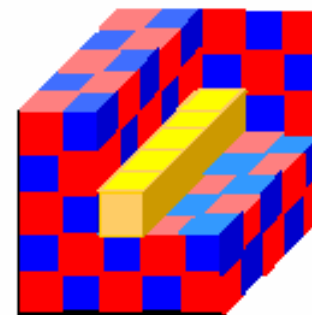


Figure 3 Iridescence in the butterfly *Morpho rhetenor*. a, Real colour image of the blue iridescence from a *M. rhetenor* wing. b, Transmission electron micrograph (TEM) images showing wing-scale cross-sections of *M. rhetenor*. c, TEM images of a wing-scale cross-section of the related species *M. didius* reveal its discretely configured multilayers. The high occupancy and high layer number of *M. rhetenor* in b creates an intense reflectivity that contrasts with the more diffusely coloured appearance of *M. didius*, in which an overlying second layer of scales effects strong diffraction⁴. Bars, a, 1 cm; b, 1.8 μm; c, 1.3 μm.

Photonic crystals



Light cavities

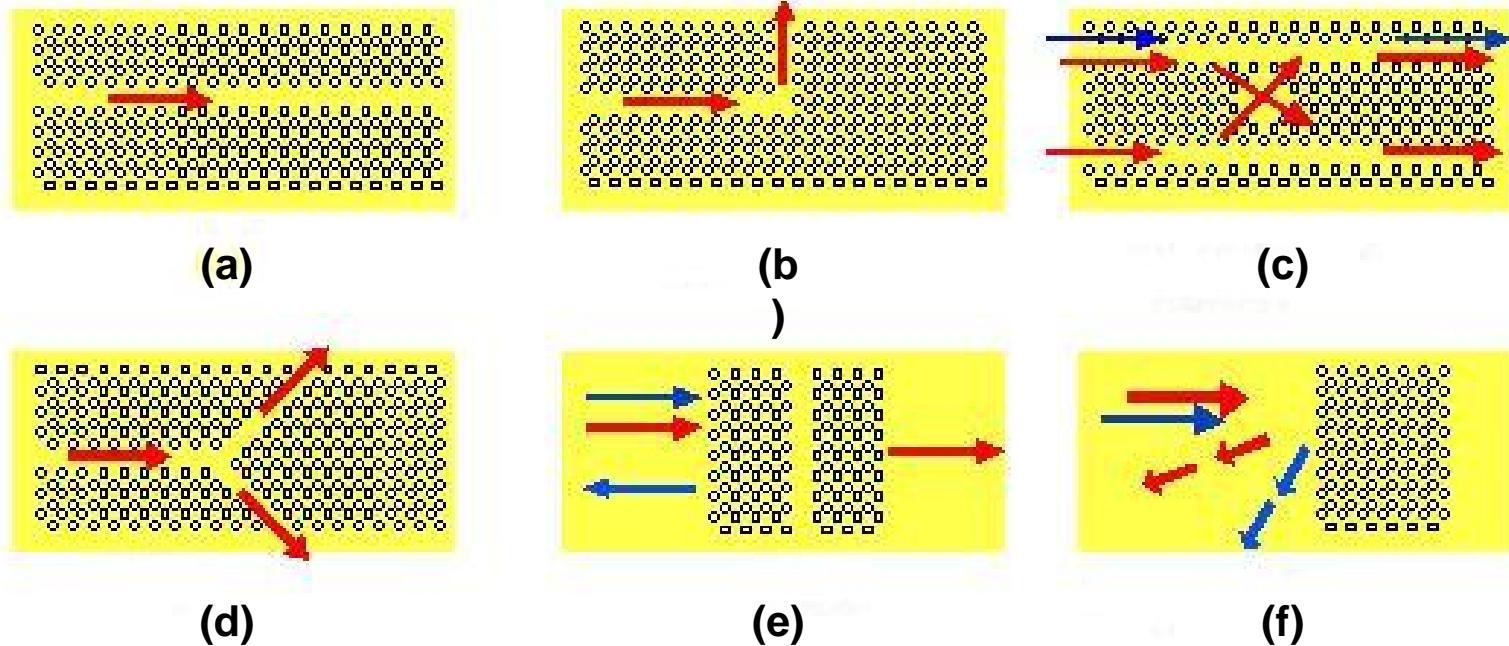


Light waveguides
('wires')

Periodic electromagnetic media

Photonic bandgap: optical insulator

Photonic bandgap waveguides



a : guide

b : sharp bend

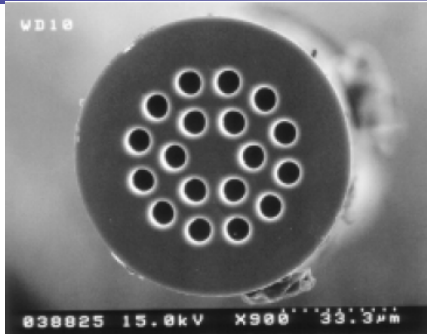
c : add/drop

d : Y-coupler

e : filter

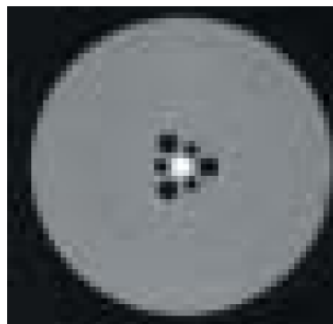
f : dispersive element

Holey fibers



Mitsubishi Cable

클래딩 지름	80μm
유효 코어 모드 지름	11.5 μm
전송 손실 (1550nm)	0.35dB/km
허용 곡률 반경	7.5mm
밴딩 손실 (1550nm) Φ 15mm × 10 turn	<0.1dB



Fujikura

FutureGuide®-SR15
→ 허용 곡률 반경 15 mm

FutureGuide®-SR7.5
→ 허용 곡률 반경 7.5 mm

Two categories of diffractive optics

Vectorial diffractive optics

1. Inhomogeneous medium
(photonic crystals, holograms,
plasmonic devices)
2. Small scale structures ($< 10\lambda$)

- Electromagnetic theory
- Non-paraxial regime
- Rigorous modeling of
diffractive elements

Scalar diffractive optics

1. Homogeneous medium
(free space)
2. Large scale structures
($> 10\lambda$)

- Scalar diffraction theory
- Paraxial regime
- Approximate modeling of
diffractive elements



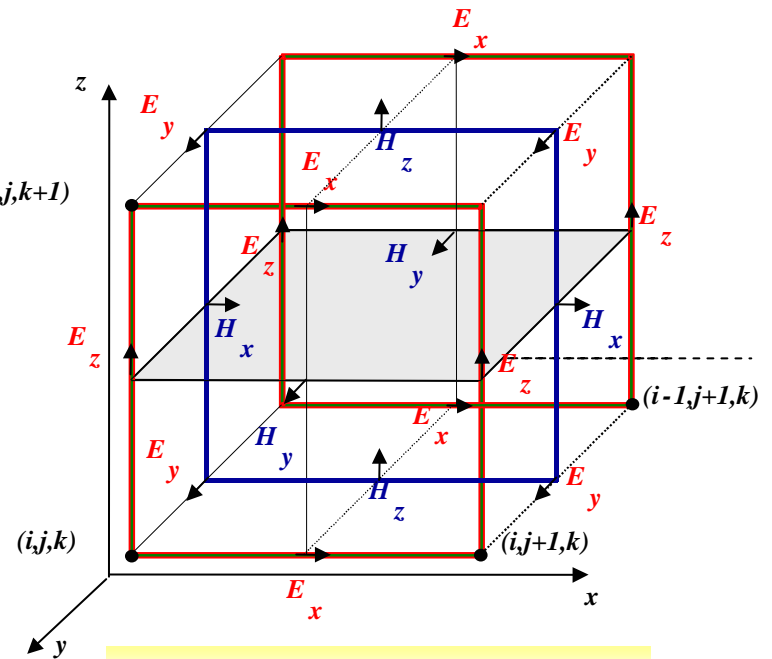
Finite-difference time-domain (FDTD) method

- FDTD is a rigorous analysis method with widely applications from nano- to all length-scales using the Maxwell's equations and curl equations

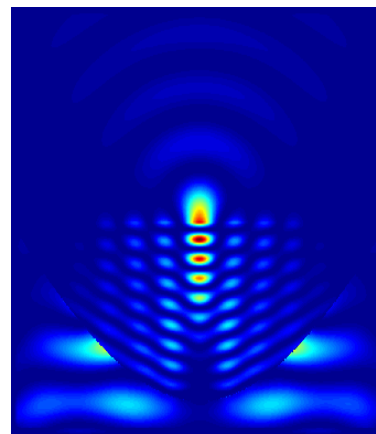
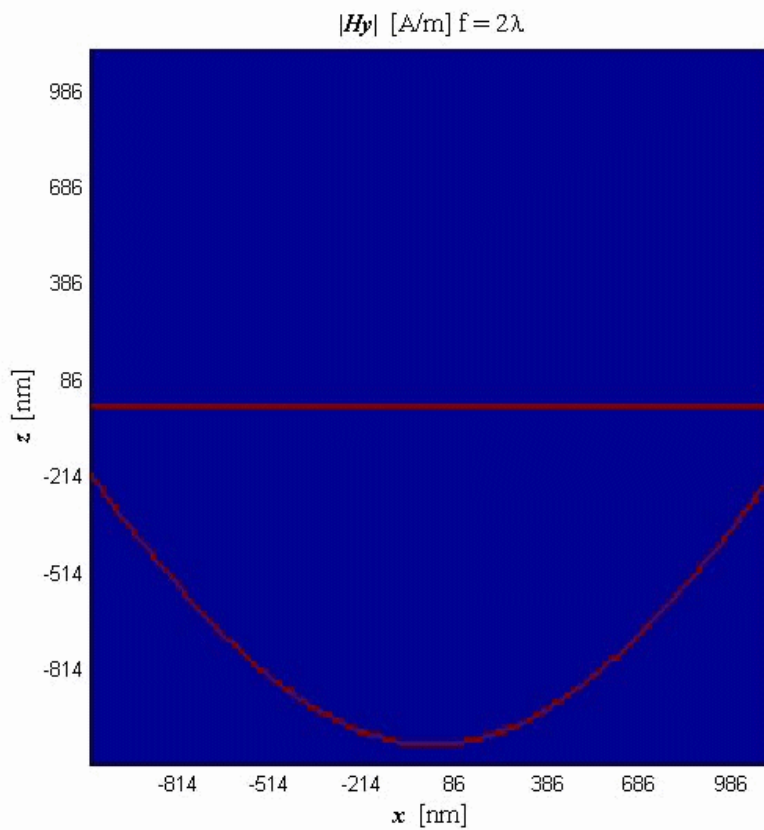
$$\frac{\partial E_x}{\partial t} = \frac{1}{\epsilon_x} \left(\frac{\partial H_y}{\partial z} - \frac{\partial H_z}{\partial y} - \sigma_x^* E_x \right) \quad \frac{\partial H_x}{\partial t} = \frac{1}{\mu_x} \left(\frac{\partial E_y}{\partial z} - \frac{\partial E_z}{\partial y} - \sigma_x^* H_x \right)$$

$$\frac{\partial E_y}{\partial t} = \frac{1}{\epsilon_y} \left(\frac{\partial H_z}{\partial x} - \frac{\partial H_x}{\partial z} - \sigma_y^* E_y \right) \quad \frac{\partial H_y}{\partial t} = \frac{1}{\mu_y} \left(\frac{\partial E_z}{\partial x} - \frac{\partial E_x}{\partial z} - \sigma_y^* H_y \right)$$

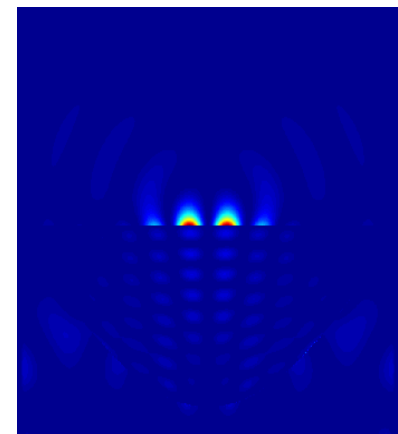
$$\frac{\partial E_z}{\partial t} = \frac{1}{\epsilon_z} \left(\frac{\partial H_x}{\partial y} - \frac{\partial H_y}{\partial x} - \sigma_z^* E_z \right) \quad \frac{\partial H_z}{\partial t} = \frac{1}{\mu_z} \left(\frac{\partial E_x}{\partial y} - \frac{\partial E_y}{\partial x} - \sigma_z^* H_z \right)$$



Solid immersion lens simulation (FDTD)



Ex – component



Ey – component

Extension to three-dimensional solid immersion lens nano-focusing for high density optical memory

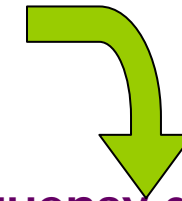
Frequency domain method for the Maxwell equations

Homogeneous Maxwell equations in the spatial domain

$$\nabla \times \underline{E} = jw\mu_0\mu(x, y, z)(\hat{x}H_x + \hat{y}H_y + \hat{z}H_z)$$

$$\nabla \times \underline{H} = -jw\varepsilon_0\varepsilon(x, y, z)(\hat{x}E_x + \hat{y}E_y + \hat{z}E_z)$$

Fourier transform



Homogeneous Maxwell equations in the (spatial) frequency domain

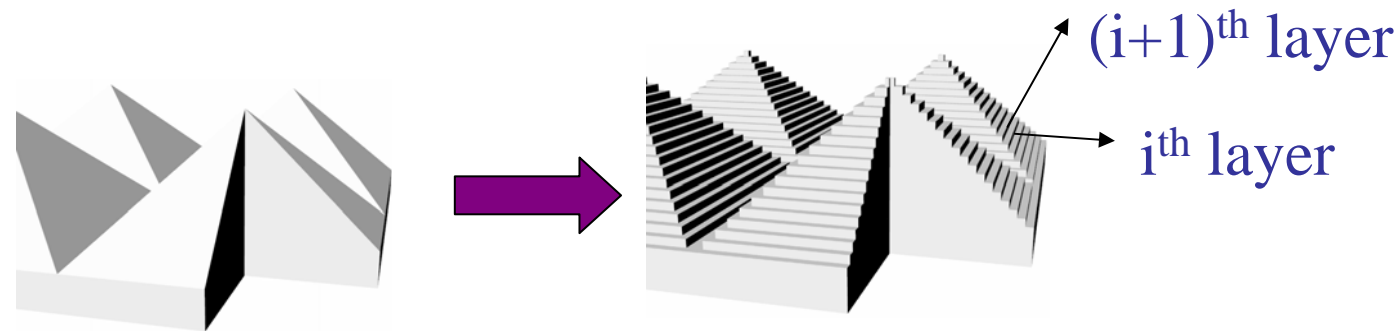
$$k_0 \begin{bmatrix} \underline{\underline{\varepsilon}}_{(x)} & 0 & 0 & 0 & 0 & 0 \\ 0 & \underline{\underline{\varepsilon}}_{(y)} & 0 & 0 & 0 & 0 \\ 0 & 0 & \underline{\underline{\varepsilon}}_{(z)} & 0 & 0 & 0 \\ 0 & 0 & 0 & \underline{\underline{\mu}}_{(x)} & 0 & 0 \\ 0 & 0 & 0 & 0 & \underline{\underline{\mu}}_{(y)} & 0 \\ 0 & 0 & 0 & 0 & 0 & \underline{\underline{\mu}}_{(z)} \end{bmatrix} \begin{bmatrix} \underline{E}_x \\ \underline{E}_y \\ \underline{E}_z \\ \underline{H}_x \\ \underline{H}_y \\ \underline{H}_z \end{bmatrix} = \begin{bmatrix} 0 & 0 & 0 & 0 & j\underline{\underline{K}}_z & -j\underline{\underline{K}}_y \\ 0 & 0 & 0 & -j\underline{\underline{K}}_z & 0 & j\underline{\underline{K}}_x \\ 0 & 0 & 0 & j\underline{\underline{K}}_y & -j\underline{\underline{K}}_x & 0 \\ 0 & j\underline{\underline{K}}_z & -j\underline{\underline{K}}_y & 0 & 0 & 0 \\ -j\underline{\underline{K}}_z & 0 & j\underline{\underline{K}}_x & 0 & 0 & 0 \\ j\underline{\underline{K}}_y & -j\underline{\underline{K}}_x & 0 & 0 & 0 & 0 \end{bmatrix} \begin{bmatrix} \underline{E}_x \\ \underline{E}_y \\ \underline{E}_z \\ \underline{H}_x \\ \underline{H}_y \\ \underline{H}_z \end{bmatrix}$$

The Maxwell equations in the spatial domain have partial differential operators. But Maxwell equations in the frequency domain are described by several algebraic equations.



Rigorous coupled wave analysis (RCWA)

Structure modeling (staircase approximation)



Fourier representation of the permittivity of the i^{th} layer

$$\underline{\epsilon}^{(i)}(x, y) = \sum_{g,h} \epsilon_{gh}^{(i)} \exp \left[j(G_{x,g}x + G_{y,h}y) \right]$$

Fourier representation of the EM fields in the i^{th} layer

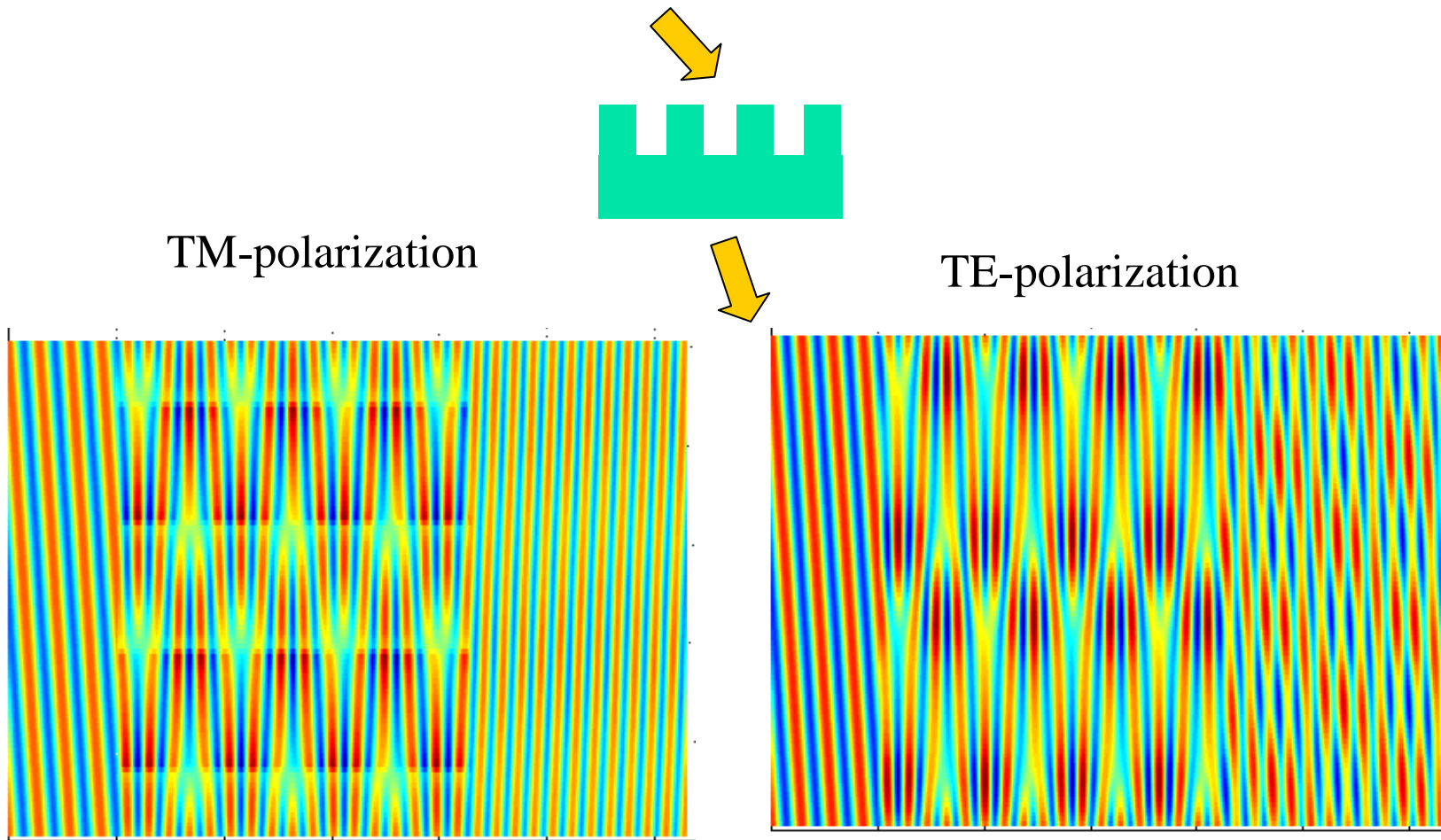
$$\underline{E}^{(i)} = \sum_{m=-M}^M \sum_{n=-N}^N \left[\underline{x} S_{x,mn}^{(i)}(z) + \underline{y} S_{y,mn}^{(i)}(z) + \underline{z} S_{z,mn}^{(i)}(z) \right] \exp \left[j(k_{x,m}x + k_{y,n}y) \right]$$

$$\underline{H}^{(i)} = j \sqrt{\frac{\epsilon_0}{\mu_0}} \sum_{m=-M}^M \sum_{n=-N}^N \left[\underline{x} U_{x,mn}^{(i)}(z) + \underline{y} U_{y,mn}^{(i)}(z) + \underline{z} U_{z,mn}^{(i)}(z) \right] \exp \left[j(k_{x,m}x + k_{y,n}y) \right]$$

The boundary conditions between adjacent layers are satisfied by the S-matrix method.

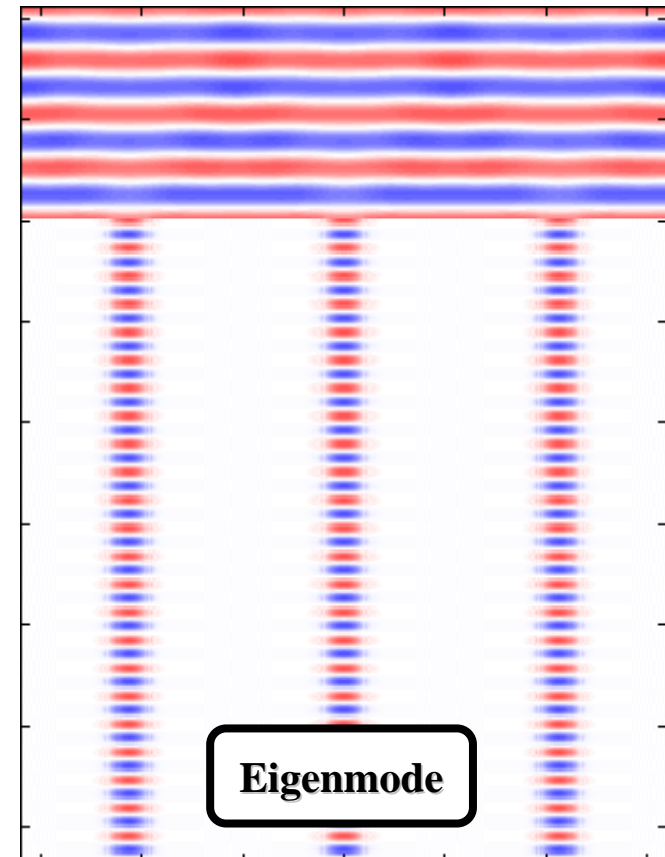
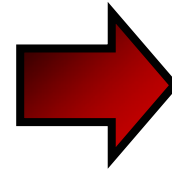
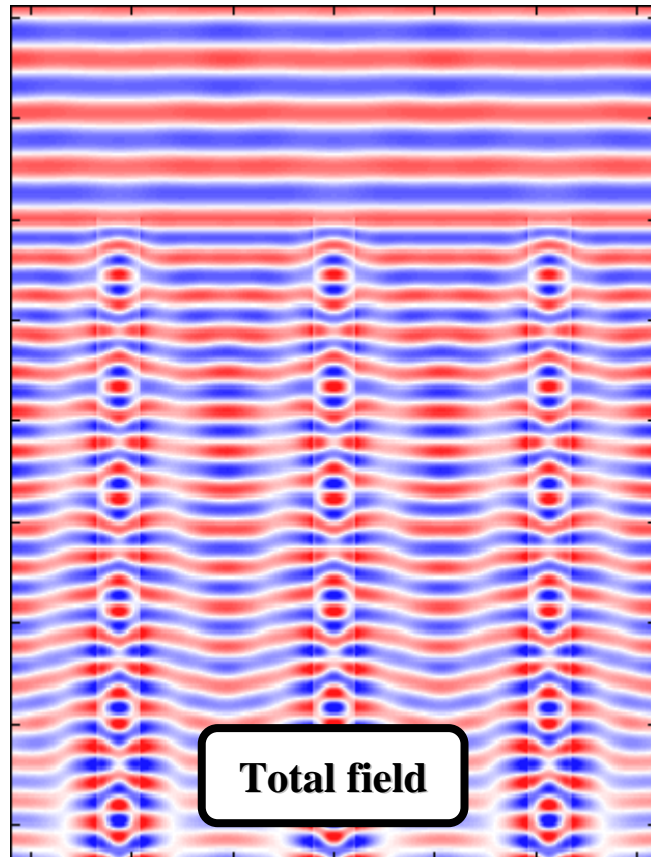
RCWA examples

2D-binary dielectric grating showing polarization-dependent diffraction



RCWA examples

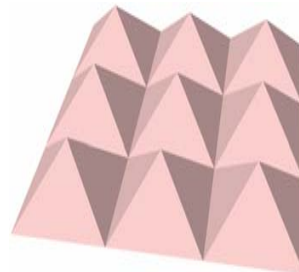
- **Modal analysis of dielectric waveguide**
 - The eigenmode extraction from total-field by observing the eigenvalue.



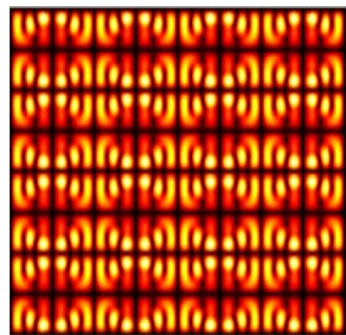
RCWA examples

3D micro-pyramid structure (15 level staircase approximation)

Wavelength(λ)=532nm
Period=3 λ , Height=6 λ
Normal incidence

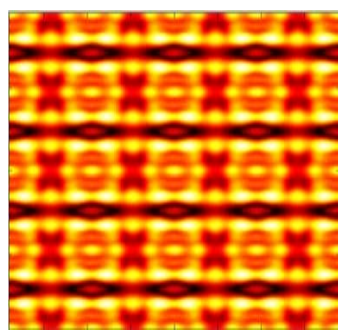


$|E_y|$

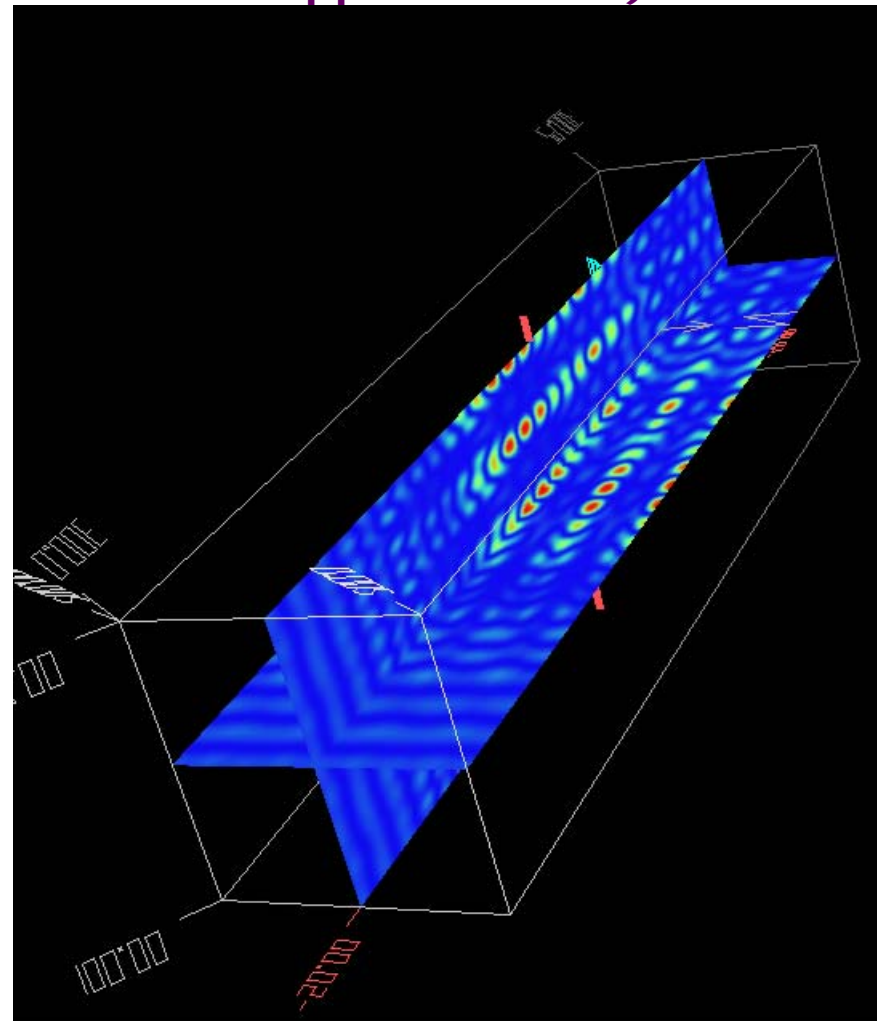


x-y crosssection

$|E_x|$

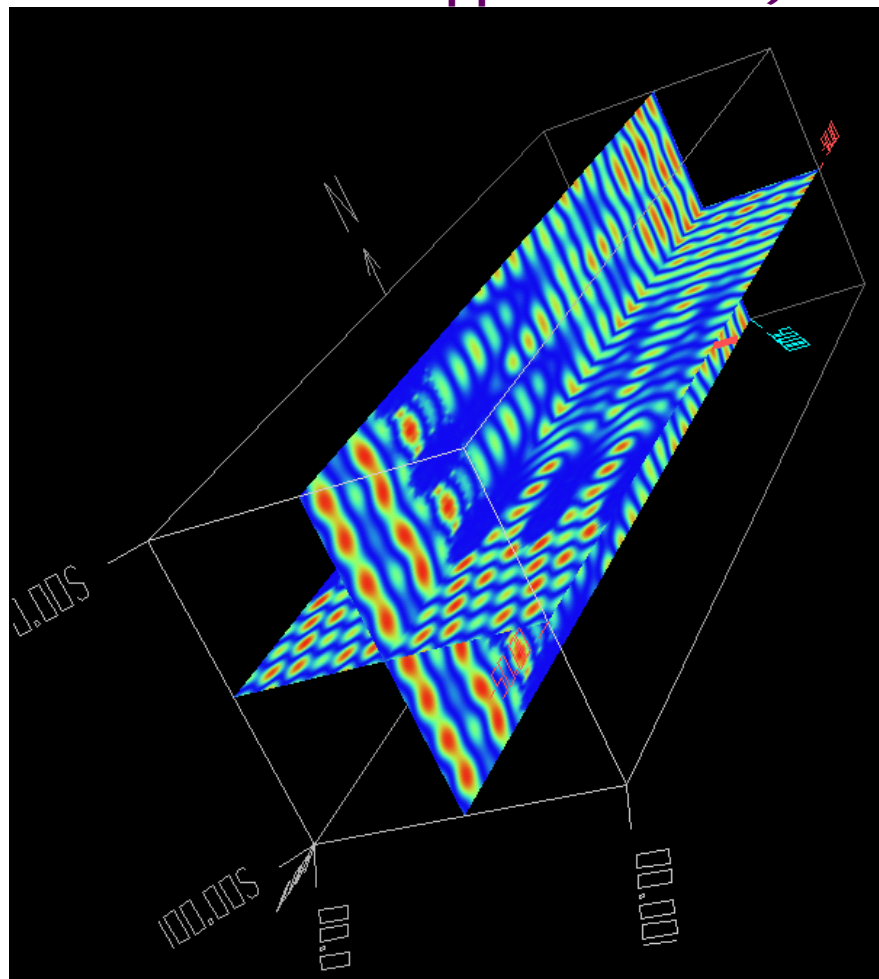
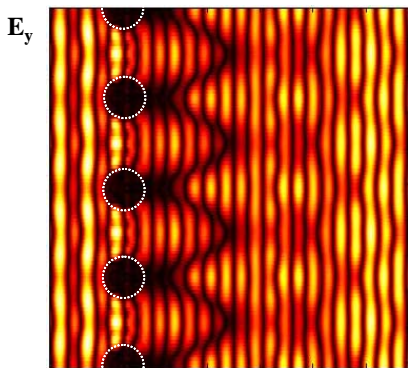
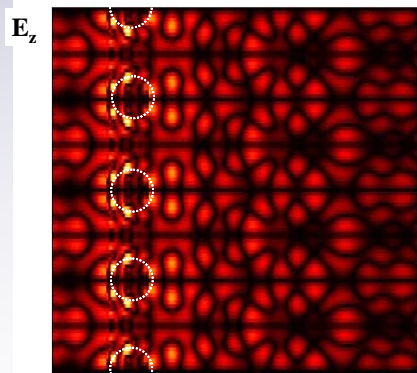
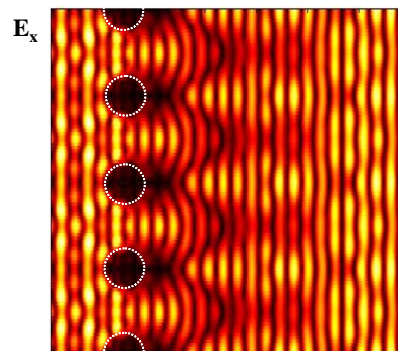
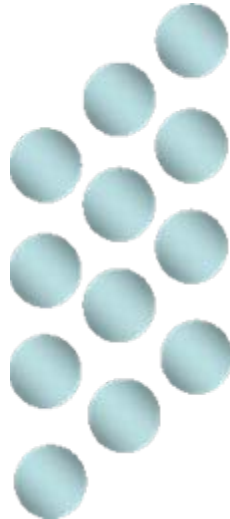


x-y crosssection



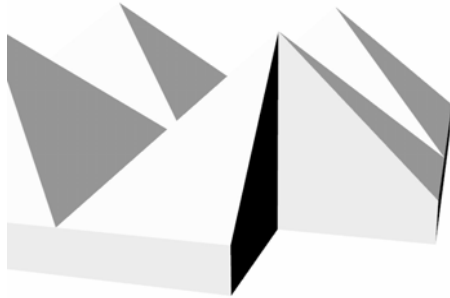
RCWA examples

3D micro-metal-sphere structure (15 level staircase approximation)



Pseudo-Fourier modal analysis (PFMA)

Structure modeling (3D Fourier series)



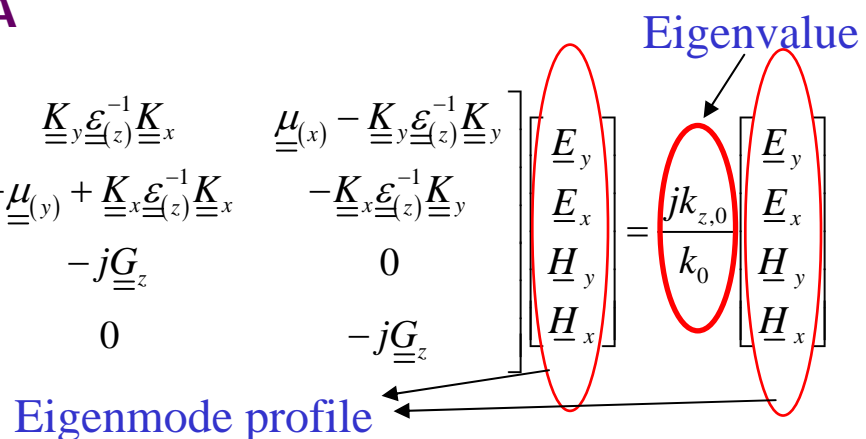
$$\mathcal{E}(x, y, z) = \sum_{s=-2M}^{2M} \sum_{t=-2N}^{2N} \sum_{p=-2H}^{2H} \tilde{\mathcal{E}}_{stp} \exp(j(k_{x,stp}x + k_{y,stp}y + k_{z,stp}z))$$

Pseudo-Fourier representation of the E-M field

$$\tilde{\mathbf{E}}_{\mathbf{k}} = e^{j(k_{x,0}x + k_{y,0}y + k_{z,0}z)} \sum_{m,n,q} (E_{x,m,n,q} \underline{x} + E_{y,m,n,q} \underline{y} + E_{z,m,n,q} \underline{z}) \exp(j(k_{x,mnq}x + k_{y,mnq}y + k_{z,mnq}z))$$

Maxwell equation in the PFMA

$$\begin{bmatrix} -j\underline{\underline{G}}_z & 0 & \underline{\underline{K}}_y \underline{\underline{\mathcal{E}}}_{(z)}^{-1} \underline{\underline{K}}_x & \underline{\underline{\mu}}_{(x)} - \underline{\underline{K}}_y \underline{\underline{\mathcal{E}}}_{(z)}^{-1} \underline{\underline{K}}_y \\ 0 & -j\underline{\underline{G}}_z & -\underline{\underline{\mu}}_{(y)} + \underline{\underline{K}}_x \underline{\underline{\mathcal{E}}}_{(z)}^{-1} \underline{\underline{K}}_x & -\underline{\underline{K}}_x \underline{\underline{\mathcal{E}}}_{(z)}^{-1} \underline{\underline{K}}_y \\ \underline{\underline{K}}_y \underline{\underline{\mu}}_{(z)}^{-1} \underline{\underline{K}}_x & \underline{\underline{\mathcal{E}}}_{(x)} - \underline{\underline{K}}_y \underline{\underline{\mu}}_{(z)}^{-1} \underline{\underline{K}}_y & -j\underline{\underline{G}}_z & 0 \\ -\underline{\underline{\mathcal{E}}}_{(y)} + \underline{\underline{K}}_x \underline{\underline{\mu}}_{(z)}^{-1} \underline{\underline{K}}_x & -\underline{\underline{K}}_x \underline{\underline{\mu}}_{(z)}^{-1} \underline{\underline{K}}_y & 0 & -j\underline{\underline{G}}_z \end{bmatrix}$$

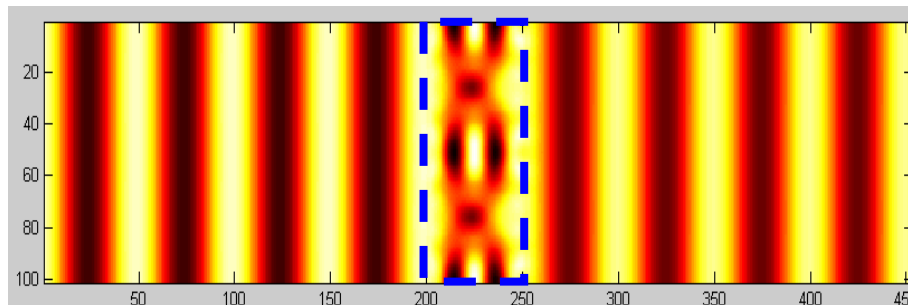
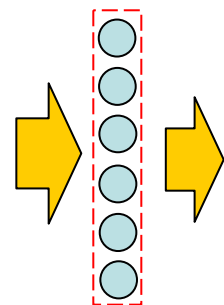


PFMA example

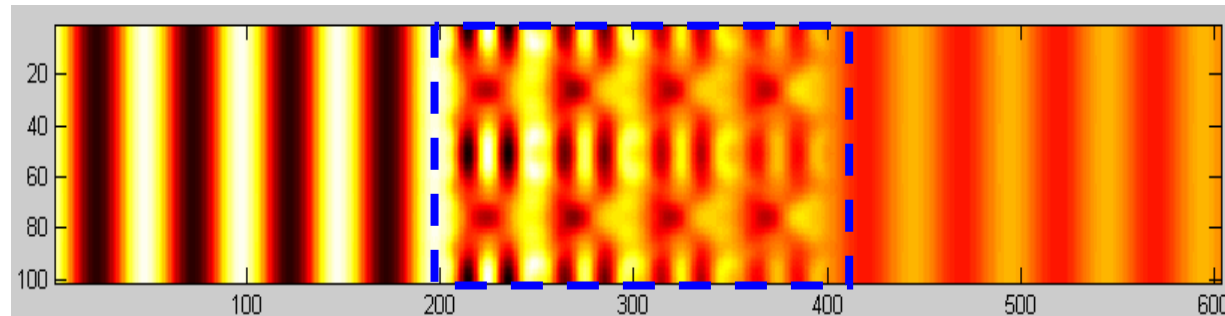
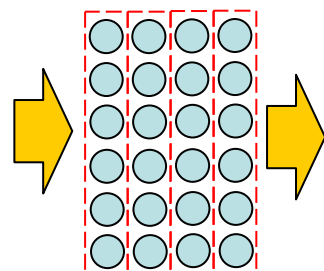
Longitudinally periodic and finite 2D photonic crystals

$$\mathbf{E} = \sum_g C_g \tilde{\mathbf{E}}_k$$

Total field distribution is a superposition of pseudo-Fourier eigenmodes with appropriate coupling coefficients.



Wavelength(λ)=532nm
Period=1.2 λ , radius=0.4 λ
Normal incidence



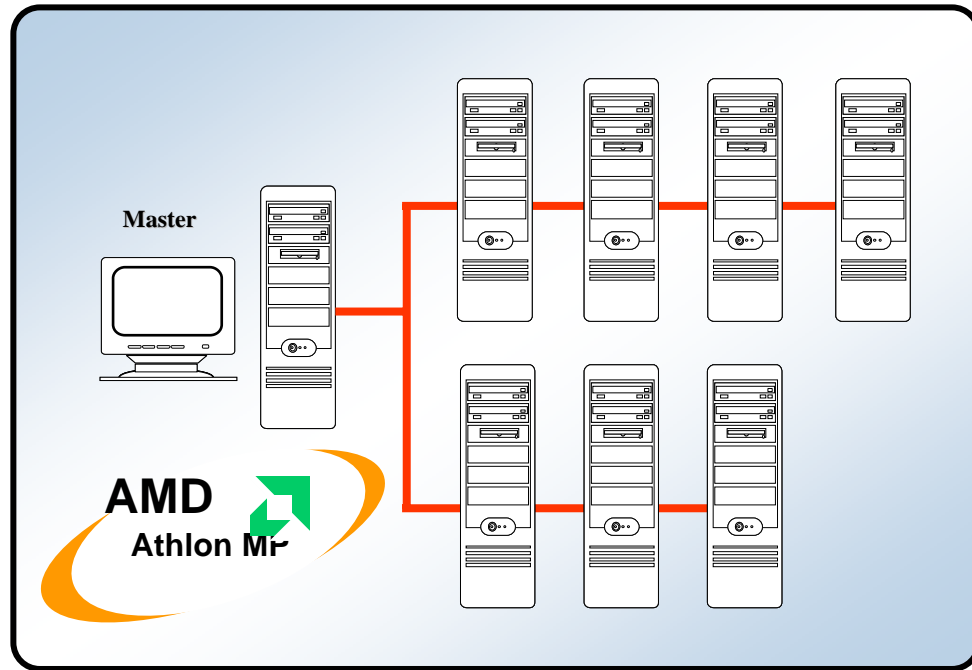
Comparison

	FDTD	RCWA	PFMA
Domain	Space	Frequency	Frequency
Field representation	Finite-difference method	Piles of truncated 2D-pseudo-Fourier series	Truncated 3D-pseudo-Fourier series
Structure modeling	Mesh-structure	Staircase approximation & piles of 2D-Fourier series	3D-Fourier series (no staircase approximation)
Aperiodic structure Analysis	Yes	No (If using PML, yes)	No (If using PML, yes)
Evanescence field analysis	No (Cannot separate)	Yes	Yes
Modal analysis	No	No	Yes
Computation cost	Very huge	Large	Huge



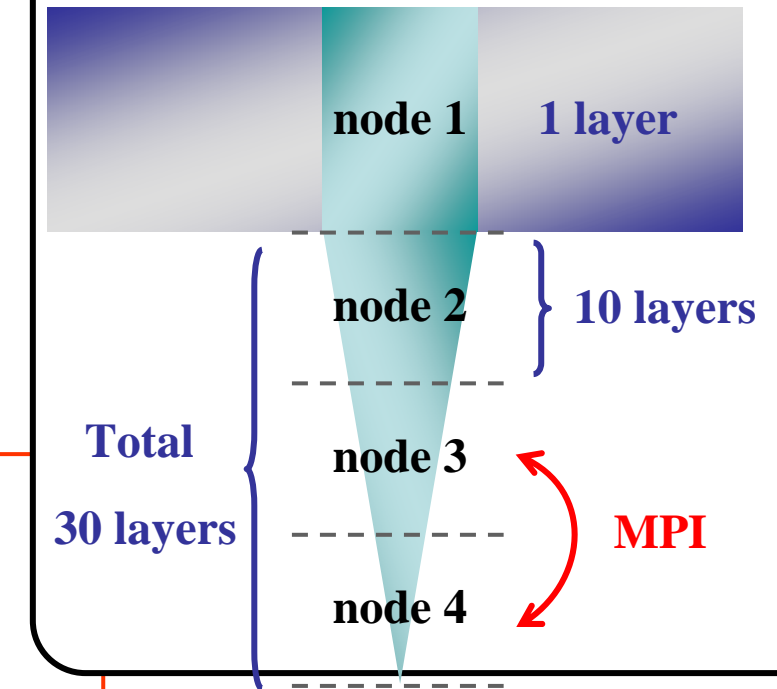
Parallel computing

Parallel computing system



Total 4 nodes

node 1 : master / node 2,3,4 : slave

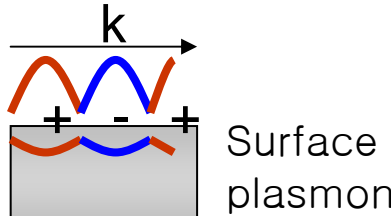
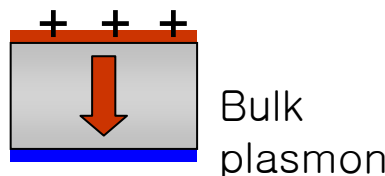


- Parallel computation based on Linux MPI
- 16 × AMD MP 2000+ CPU
- 32G memory
- 1Gbps network
- MPI and Scalapack library for parallel linear algebra

Plasmonics

What is a plasmon?

- “Plasma-oscillation”: density fluctuation of free electrons



The Lycurgus Cup (glass)
British Museum
4th century A.D.

Green when illuminated from outside and red when illuminated from within the cup due to very small amounts of gold powder about 40 parts per million)



“Labors of the Months”
Norwich, England
ca. 1480

The ruby color is attributed to gold nanoparticles.

Surface plasmon

Surface plasmon (SP)

- EM surface-bound wave between a metal and dielectric surface (p-polarized, TM wave)
- The metal behaves like a plasma, having equal amounts of positive and negative charges, of which the electrons are mobile.
- The bound wave has an evanescent field which decays exponentially perpendicular to the surface.
- SPs can be produced by photons in the attenuated total reflection device.
- SPs have played a significant role in a variety of areas of fundamental and applied research, from surface sensitive technique to surface plasmon resonance microscopy and a wide range of photonic applications.

- Dispersion of SP

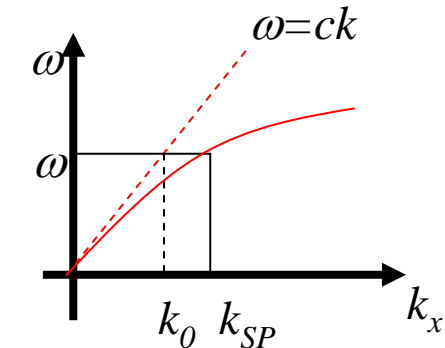
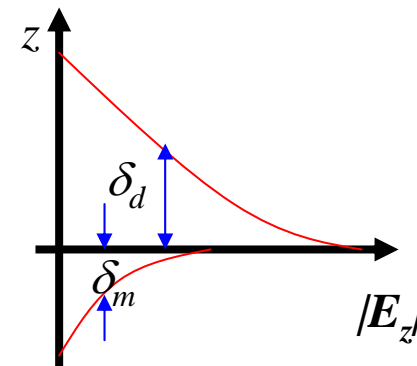
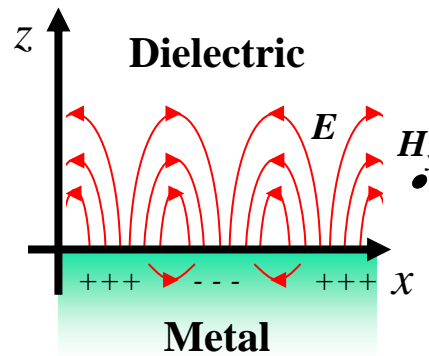
$$k_{SP} = k_0 \sqrt{\frac{\epsilon_d \epsilon_m}{\epsilon_d + \epsilon_m}} = \frac{\omega}{c} \sqrt{\frac{\epsilon_d \epsilon_m}{\epsilon_d + \epsilon_m}}$$

ex) for silver-air interface, $k_{SP} = 1.03k_0$

- Propagation length, δ_{SP}

$$\delta_{SP} = \frac{1}{2k''_{SP}} = \frac{c}{\omega} \left(\frac{\epsilon'_m + \epsilon'_d}{\epsilon'_m \epsilon'_d} \right)^{3/2} \frac{(\epsilon'_m)^2}{\epsilon''_m}$$

ex) for silver-air interface, $\delta_{SP} = 20 \mu\text{m}$

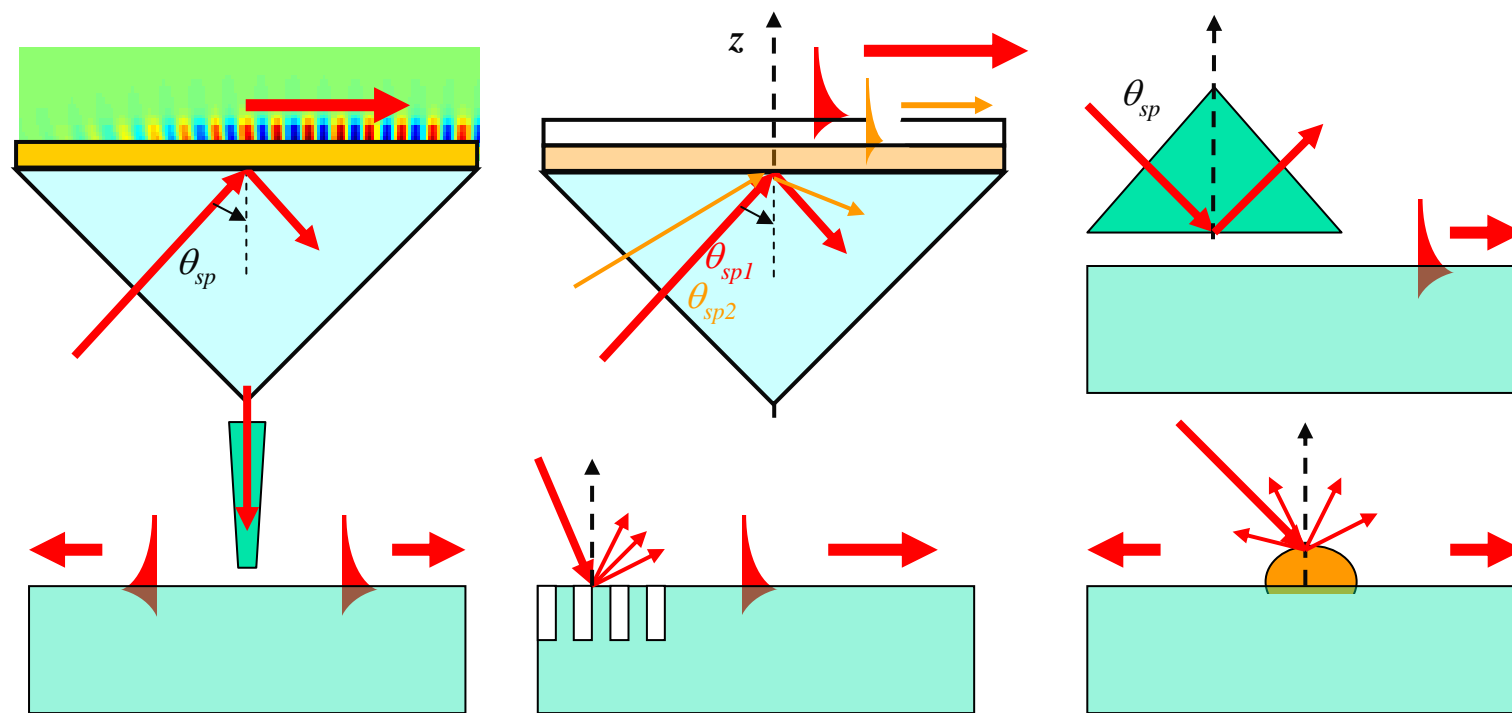


Surface charges, evanescent fields, and dispersion curve for SP mode

Surface plasmon excitation

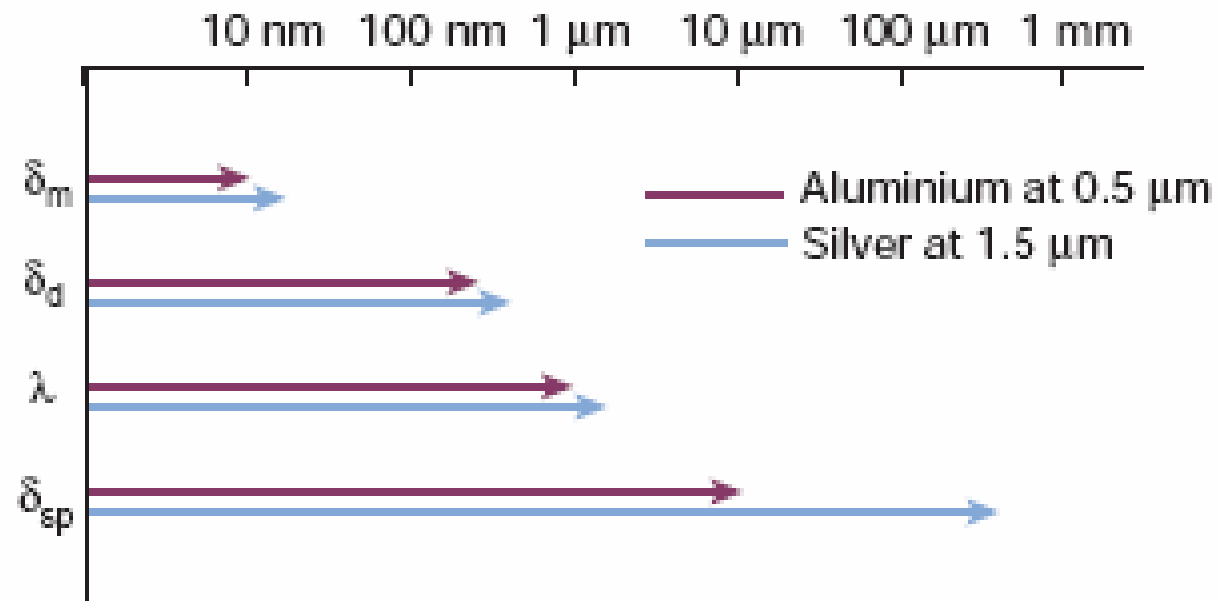
Excitation methods

- Kretschmann geometry, Otto geometry, SNOM probe
- Diffraction grating, bumped metal surfaces



SPP excitation configurations

Surface plasmon

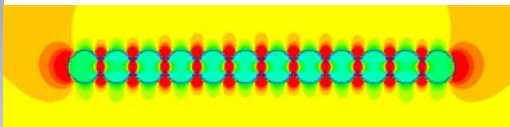


Surface plasmons in nanoparticles

Confined SPs in Nanoparticles

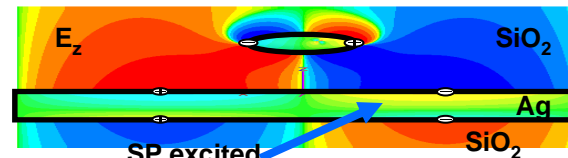
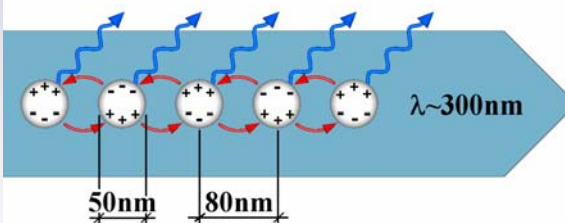
- Particle can be considered as a dipole

$$\vec{p} = 4\pi\epsilon_0 R^3 \frac{\epsilon - \epsilon_m}{\epsilon + 2\epsilon_m} \epsilon_m \vec{E}_0$$



Resonant enhancement of p if

$$|\epsilon(\omega) + 2\epsilon_m| = \text{minimum}$$



- Uniform sphere, spheroid, rod shaped metal nano-particles
- Interaction between particles, plasmonic chains
- Focusing and guidance of light at nanometer length scales

Electric polarizability of a sphere α

$$\alpha = 4\pi\epsilon_0 R^3 \frac{\epsilon - \epsilon_m}{\boxed{\epsilon + 2\epsilon_m}}$$

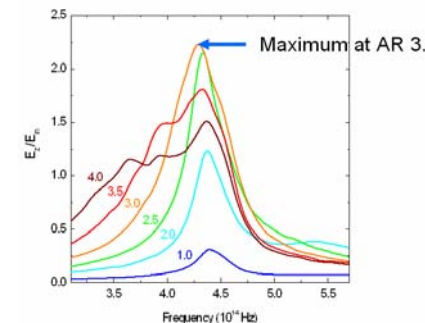
$$\epsilon = \epsilon_1(\omega) + i\epsilon_2(\omega)$$

Dielectric constant of the metal particle

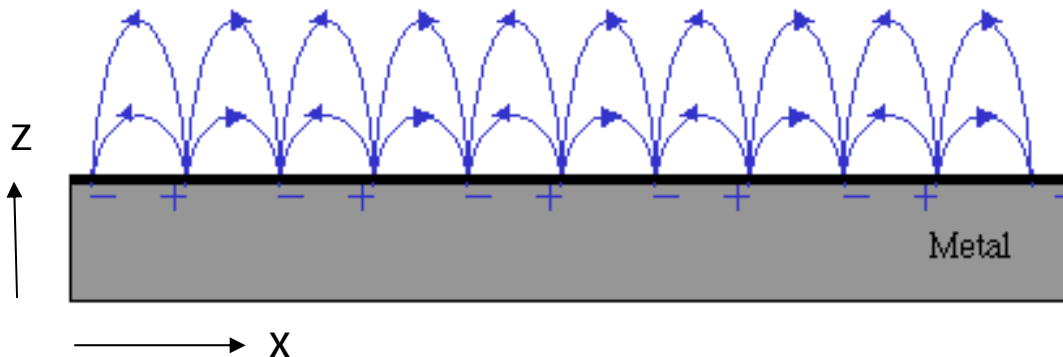
ϵ_m : Dielectric constant of the embedding medium. Usually real and taken independent of frequency.

→ Negative real dielectric constant $\epsilon_1(\omega)$

Bohren and Huffman (1983), p.136

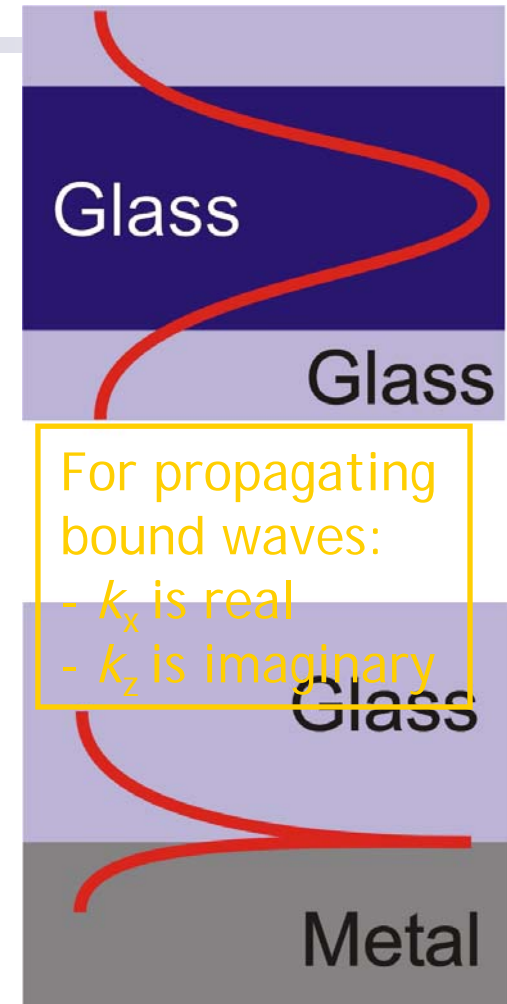


Surface plasmon polariton



$$\vec{E}_d(x, z, t) = \vec{E}_{d,0} e^{i(k_x x + k_z z - \omega t)}$$

$$\vec{E}_m(x, z, t) = \vec{E}_{m,0} e^{i(k_x x - k_z z - \omega t)}$$

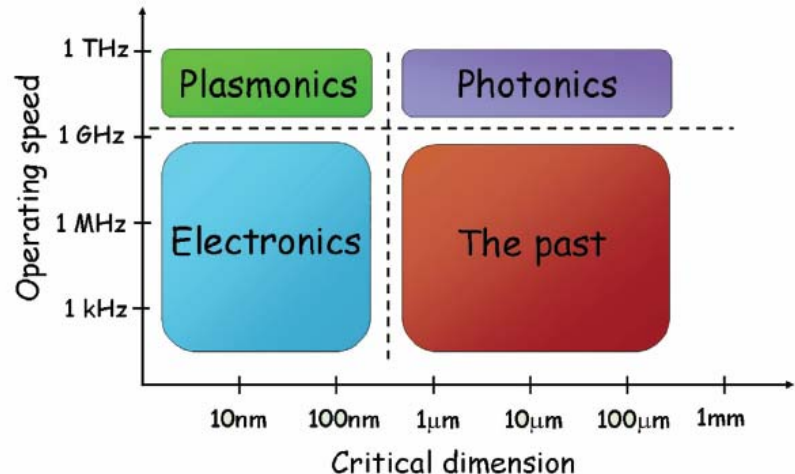


For propagating bound waves:

- k_x is real
- k_z is imaginary

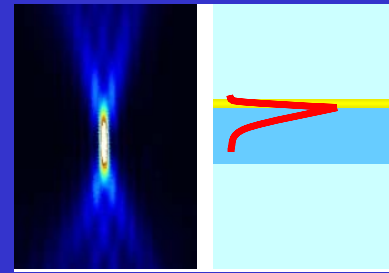
EM wave is coupled to the **plasma oscillations** of the surface charges

Plasmonics: A bridge between electronics and photonics



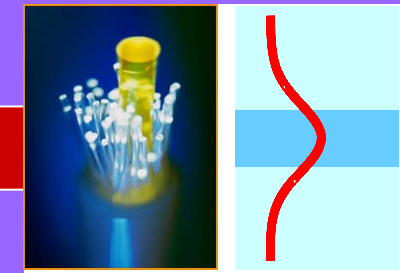
Surface plasmon

line width : ≤ 50 nm



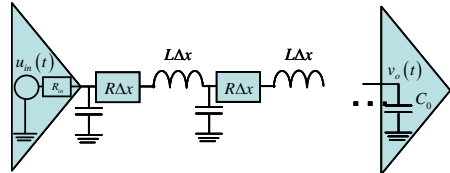
Optical waveguide

core size : ~ 10 μm



Transmission model

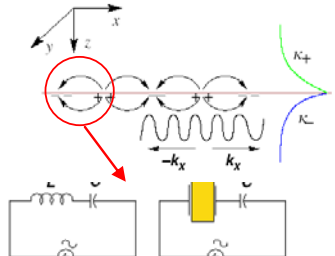
CMOS VLSI RLC transmission line interconnection



50% signal propagation delay $T_{50\%}$
(Ismail-Friedman formula)

$$T_{50\%, \text{CMOS}} \propto \frac{1}{\omega_{c, \text{CMOS}}}$$

Surface plasmon polariton wave propagation



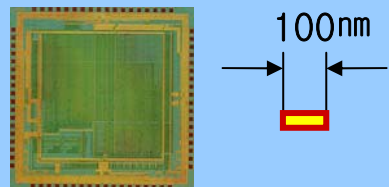
Coupled RLC resonator transmission line

$$T_{50\%, \text{SPP}} \propto \frac{1}{\omega_{c, \text{SPP}}}$$

$$T_{50\%, \text{CMOS}} > T_{50\%, \text{SPP}}$$

Semiconductor IC

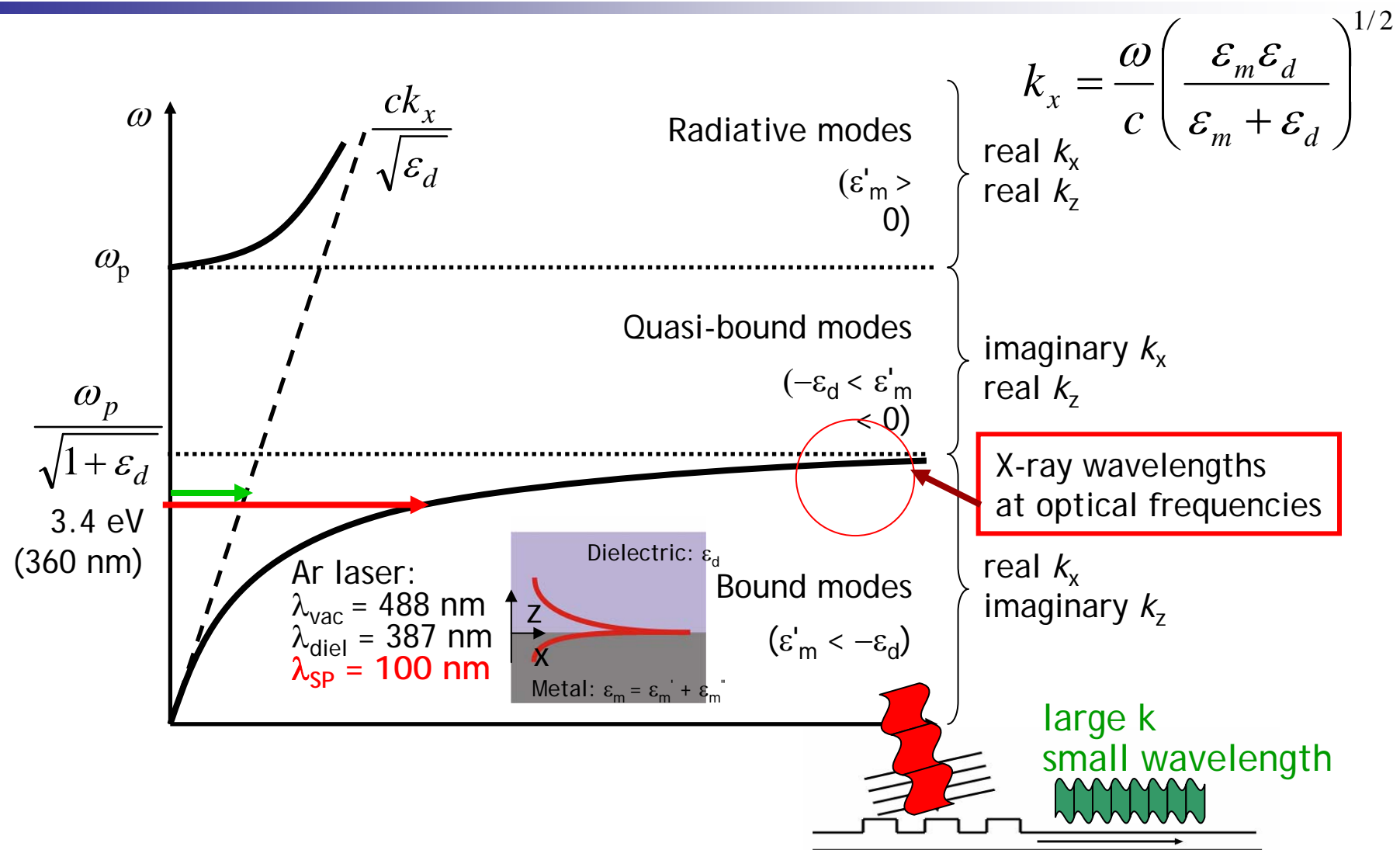
line width : ≤ 100 nm



H. Ditlbacher *et al.*, "Silver Nanowires as Surface Plasmon Resonators," Physical Review Letters 95, pp.257403, 2005.

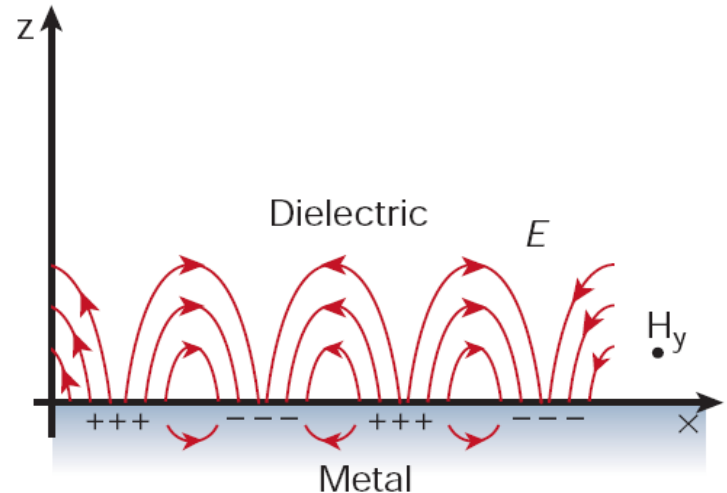
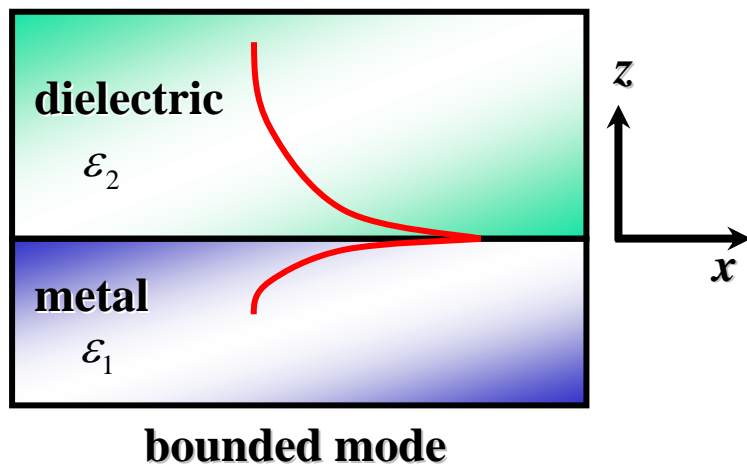


Surface plasmon dispersion relation



Surface plasmon dispersion relation

Semi-infinite metal structure



In metal, $z < 0$

$$\vec{H}_1 = (0, H_{y1}, 0) \exp[j(k_x x - k_{z1} z)]$$

$$\vec{E}_1 = (E_{x1}, 0, E_{z1}) \exp[j(k_x x - k_{z1} z)]$$

In dielectric, $z > 0$

$$\vec{H}_2 = (0, H_{y2}, 0) \exp[j(k_x x + k_{z2} z)]$$

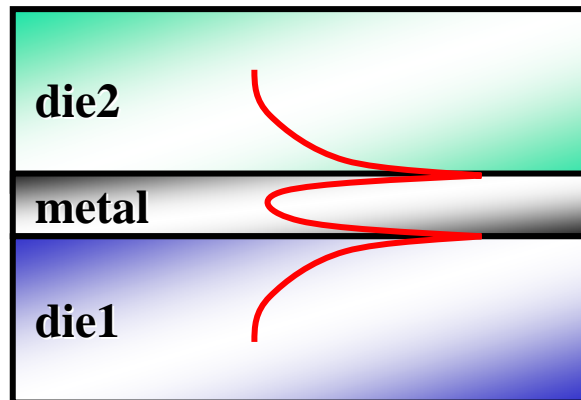
$$\vec{E}_2 = (E_{x2}, 0, E_{z2}) \exp[j(k_x x + k_{z2} z)]$$

Using the
continuity relation

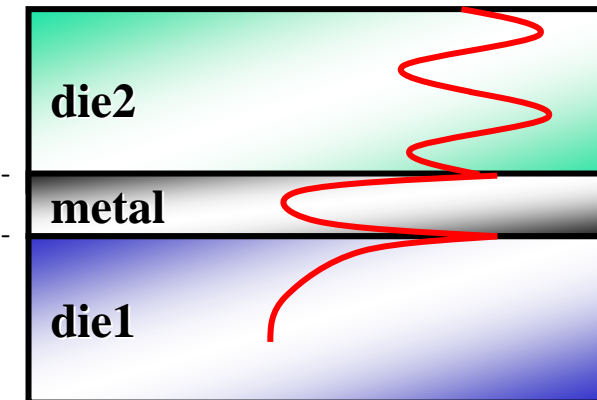
$$k_{sp} = \frac{\omega}{c_0} \sqrt{\frac{\epsilon_1 \epsilon_2}{\epsilon_1 + \epsilon_2}}$$

Surface plasmon dispersion relation

Finite metal slab structure



bound mode

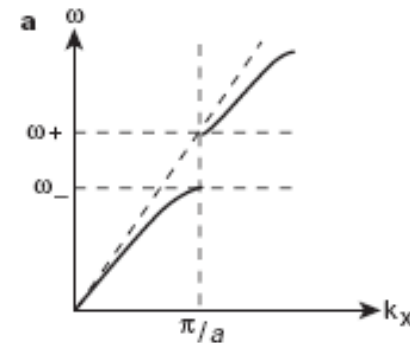
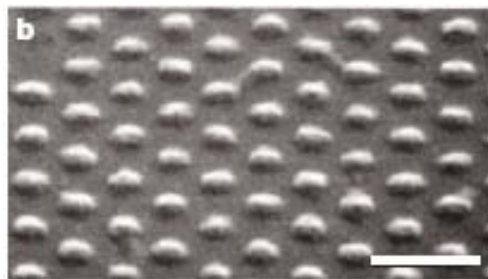


radiation mode

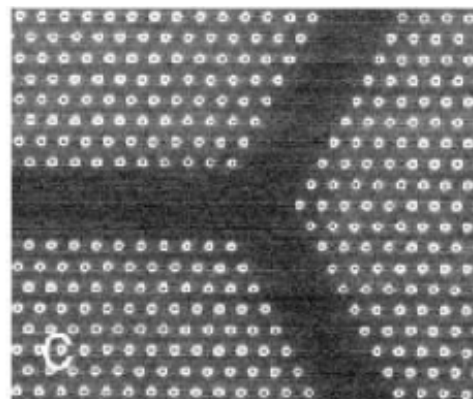
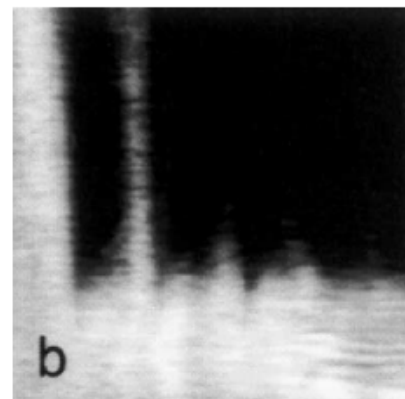
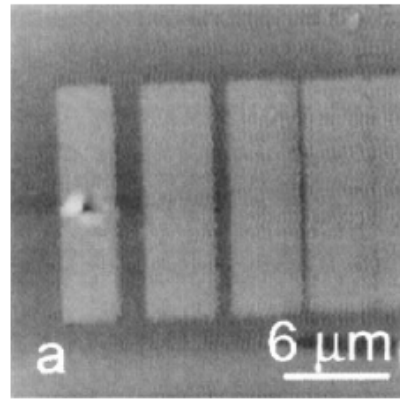
$$\text{Char. eqn. : } \left(\frac{\epsilon_m k_{z1}}{\epsilon_1 k_{zm}} + 1 \right) \left(\frac{\epsilon_m k_{z2}}{\epsilon_2 k_{zm}} + 1 \right) = \left(\frac{\epsilon_m k_{z1}}{\epsilon_1 k_{zm}} - 1 \right) \left(\frac{\epsilon_m k_{z2}}{\epsilon_2 k_{zm}} - 1 \right) \exp(-2k_{zm}d)$$

$$\text{let } f(k_x) = \left(\frac{\epsilon_m k_{z1}}{\epsilon_1 k_{zm}} + 1 \right) \left(\frac{\epsilon_m k_{z2}}{\epsilon_2 k_{zm}} + 1 \right) - \left(\frac{\epsilon_m k_{z1}}{\epsilon_1 k_{zm}} - 1 \right) \left(\frac{\epsilon_m k_{z2}}{\epsilon_2 k_{zm}} - 1 \right) \exp(-2k_{zm}d)$$

Metal surface relief gratings



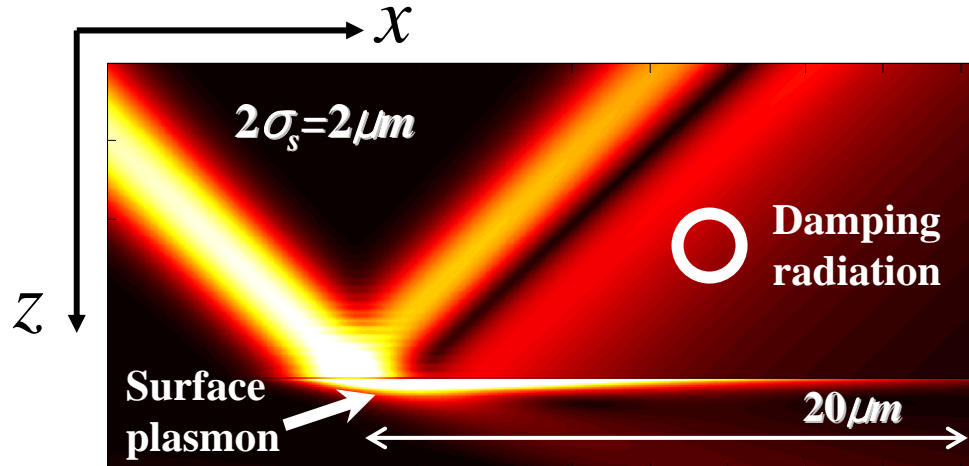
S. Kitson, PRL, 77, 2670, (1996)



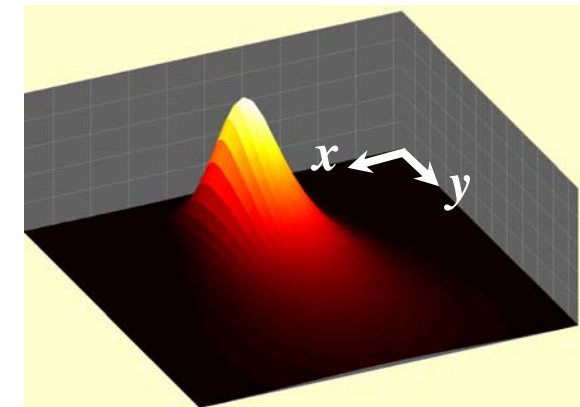
S. Bozhevolnyi, PRL, 86, 3008, (2001)

Surface plasmon excitation by Gaussian beams and pulses in TIR geometry

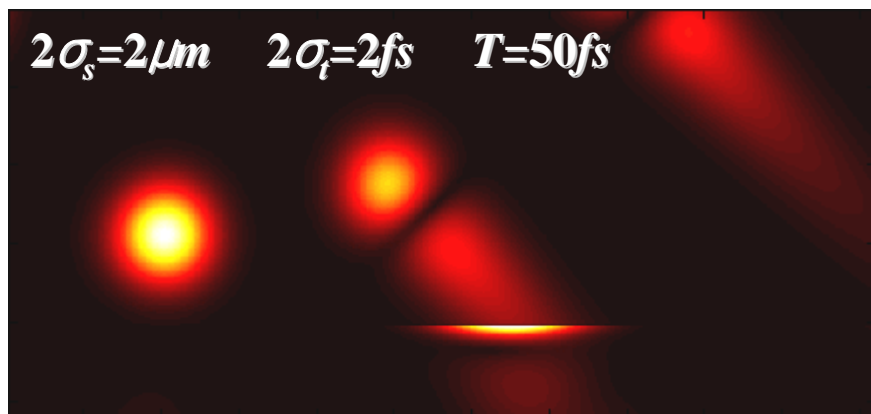
Finite metal slab structure



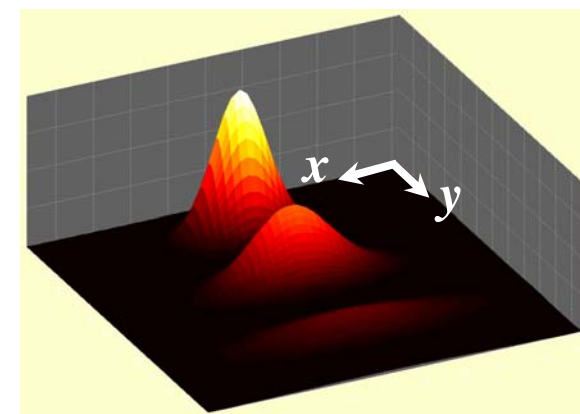
Surface plasmon excited by Gaussian beam



At metal surface

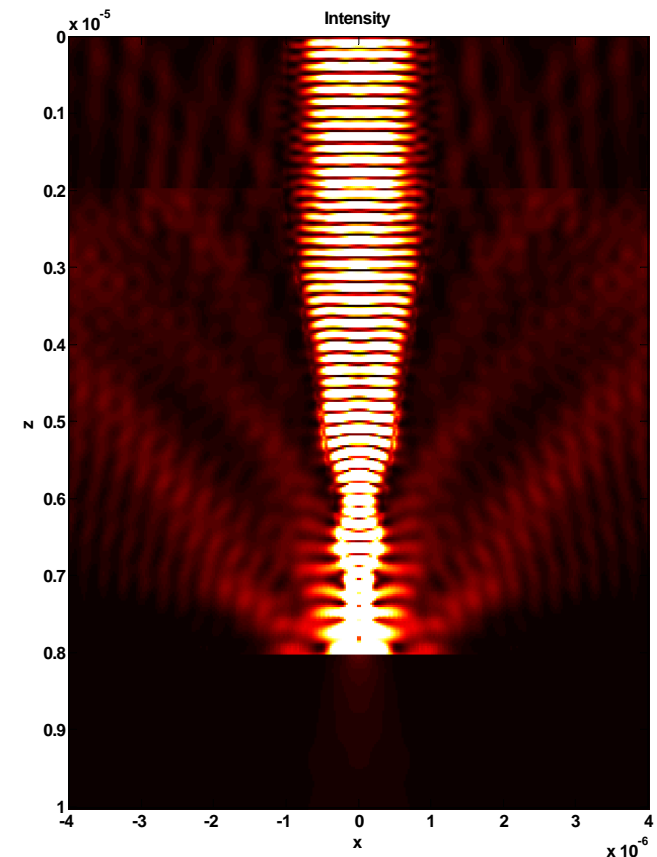
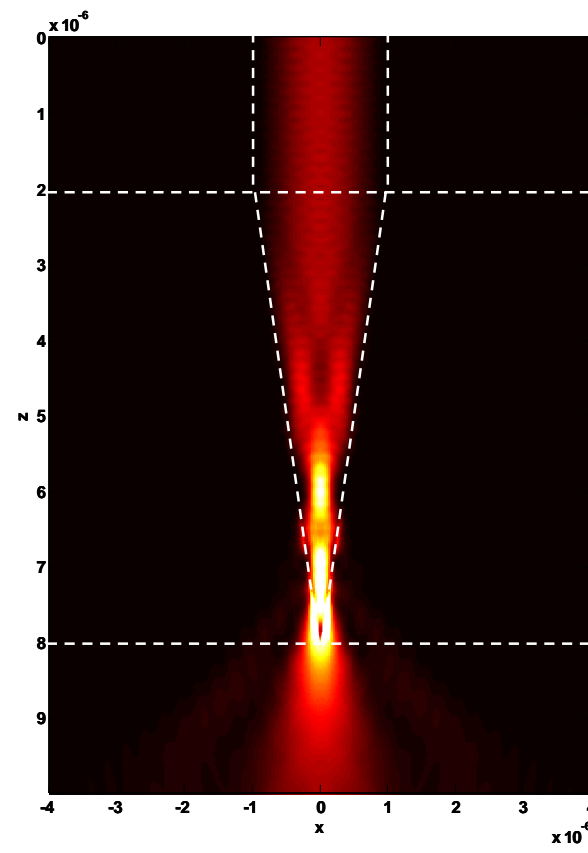
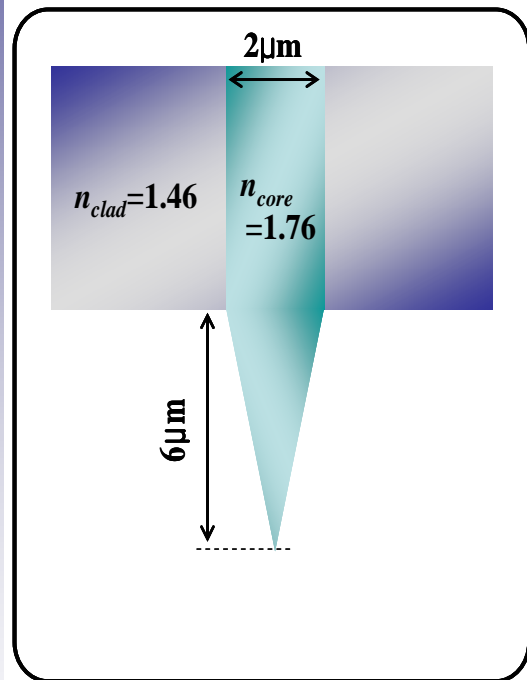


Surface plasmon excited by Gaussian pulse beam
Seoul National University

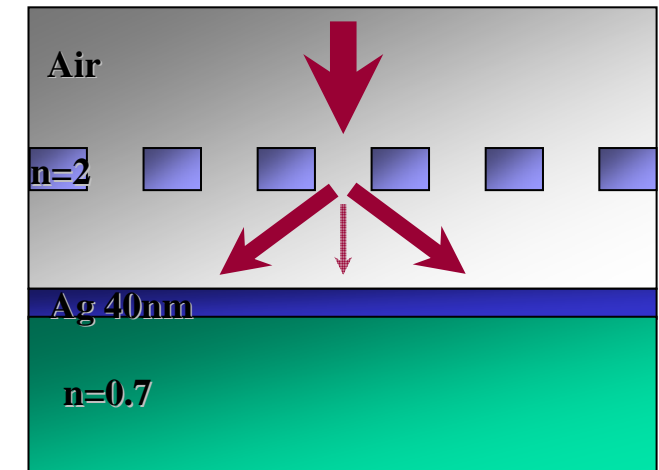
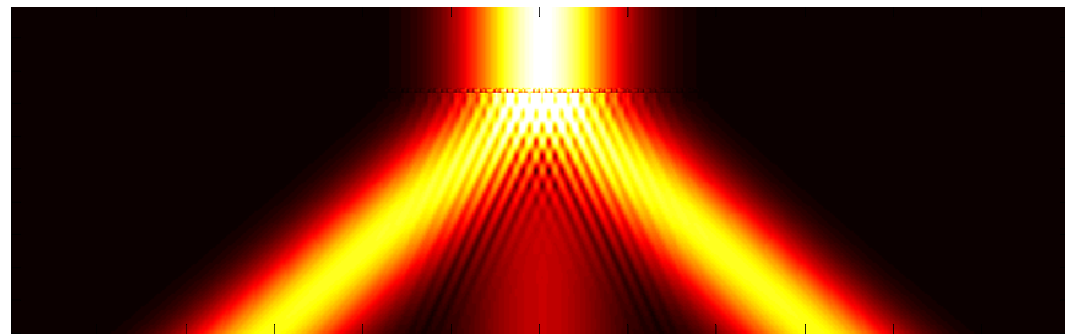
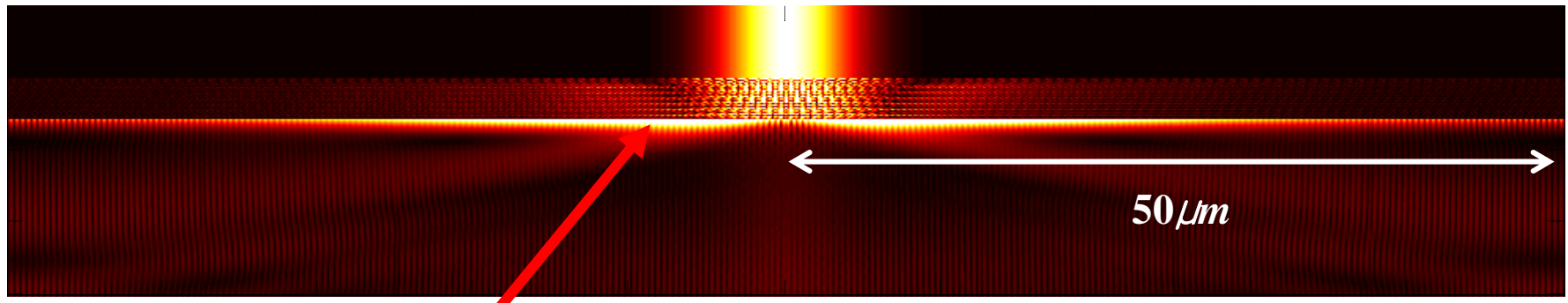


At metal surface

Surface plasmon excitation by NSOM tips

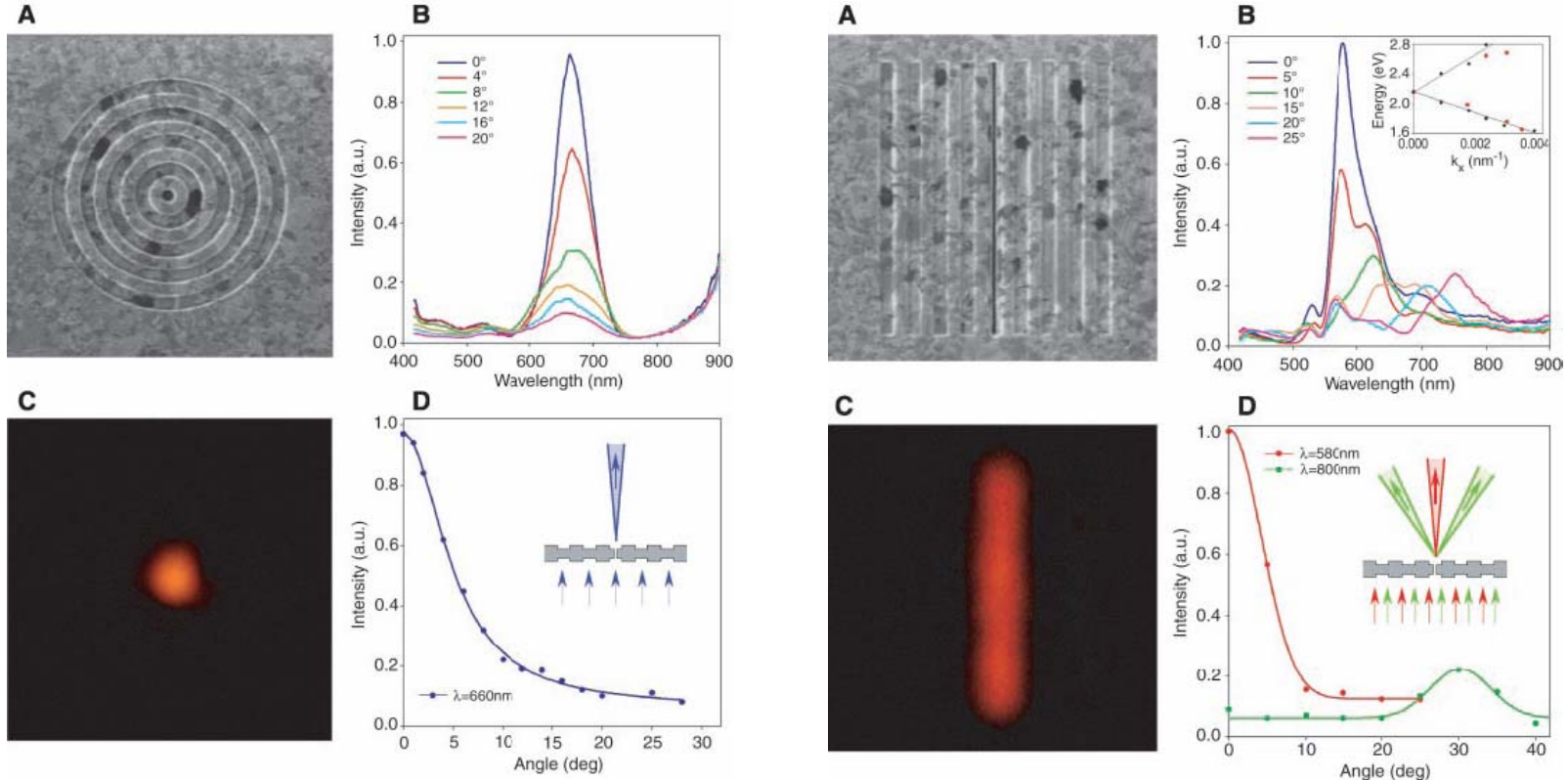


Surface plasmon excited by a normal incident focused Gaussian beam by a dielectric grating coupler



Beaming light from a subwavelength aperture

H. J. Lezec, A. Degiron, E. Devaux, R. A. Linke, L. Martin-Moreno, F. J. Garcia-Vidal, T. W. Ebbesen,
Science. vol. 297. no. 2. pp. 820-822. 2002.



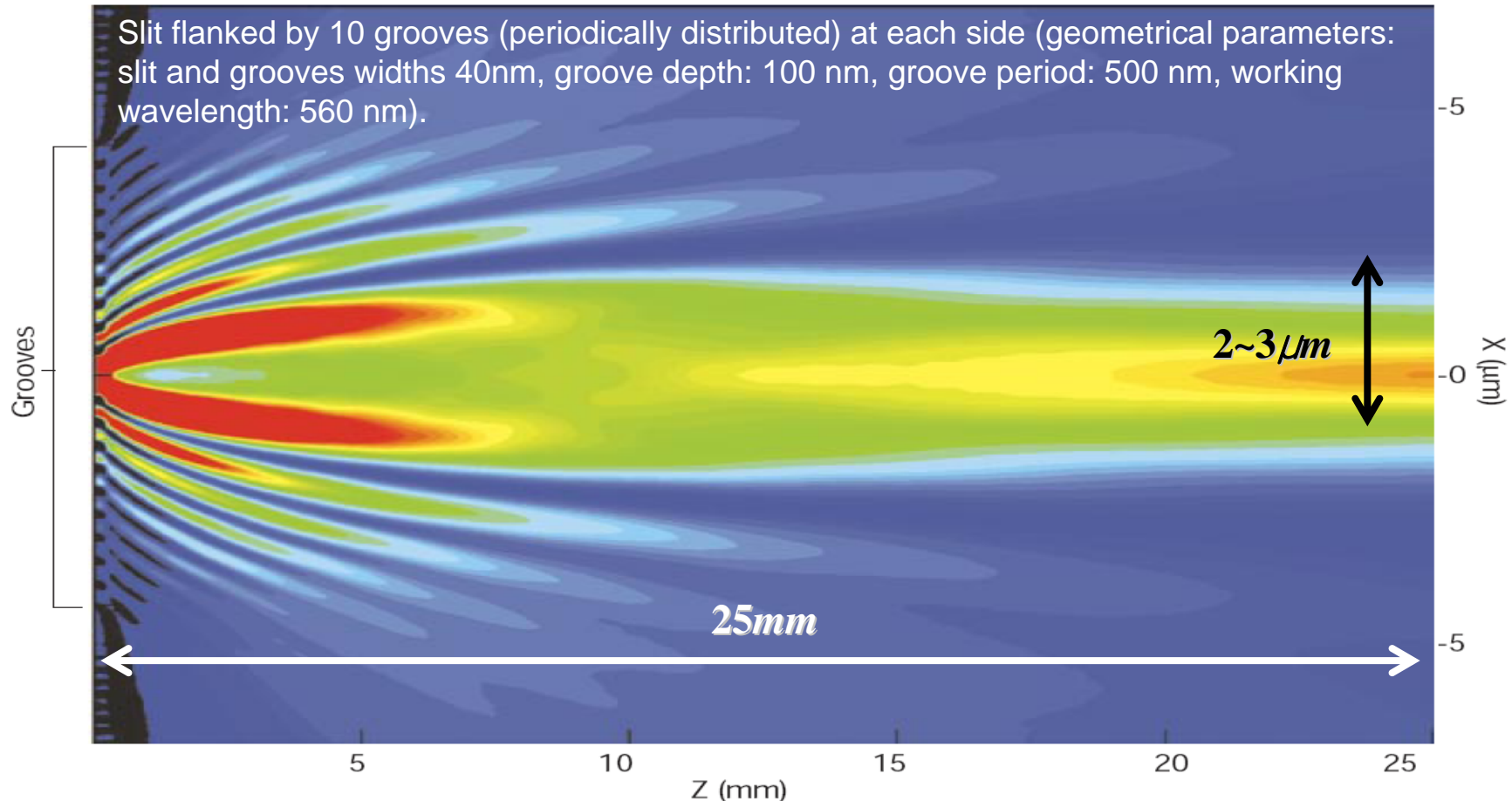
Light usually diffracts in all directions when it emerges from a subwavelength aperture, which puts a lower limit on the size of features that can be used in photonics. This limitation can be overcome by creating a periodic texture on the exit side of a single aperture in a metal film. The transmitted light emerges from the aperture as a beam with a small angular divergence



Surface plasmon subwavelength optics

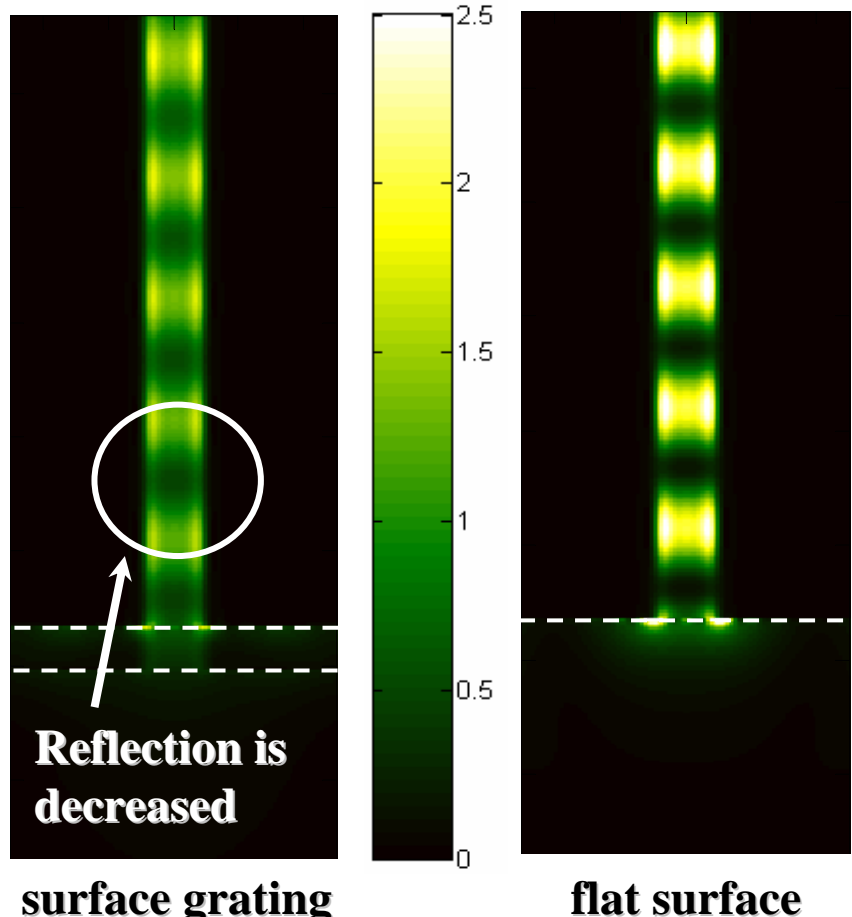
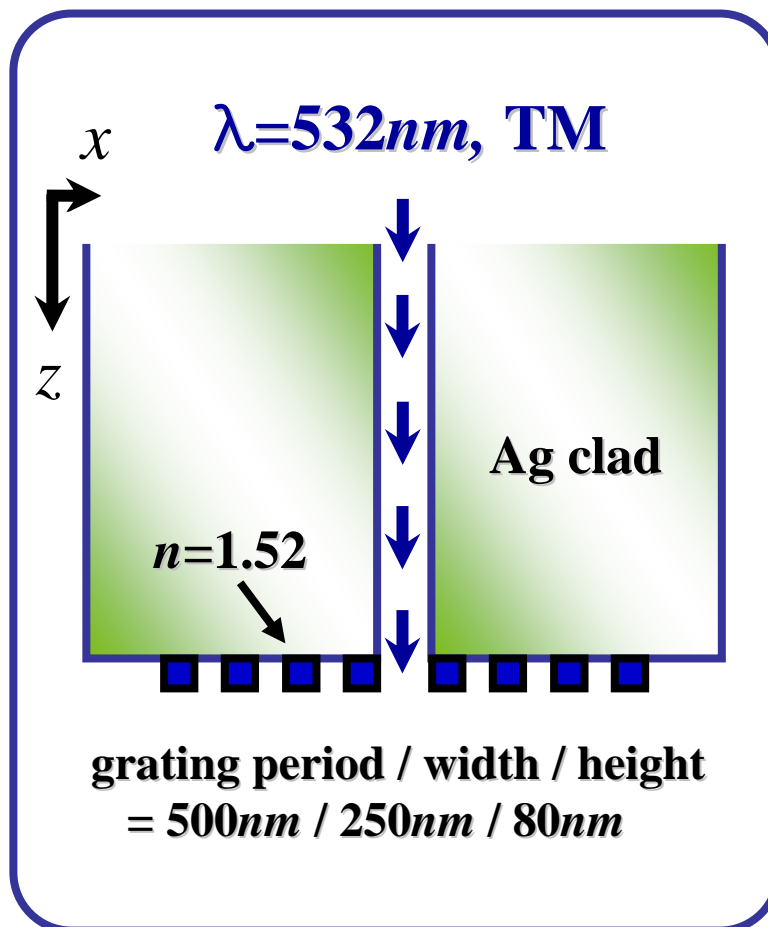
W. L. Barnes, A. Degiron, and T. W. Ebbesen, *Nature*, vol. 424, pp. 824-830, 2003.

Bull's eye structure- beaming light by subwavelength structures



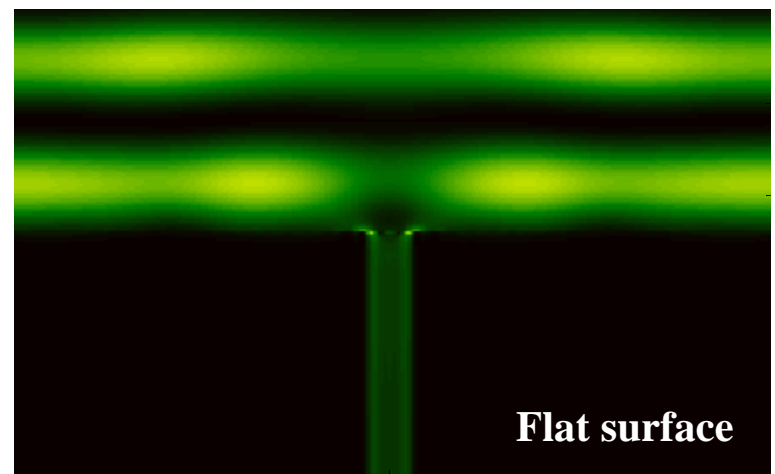
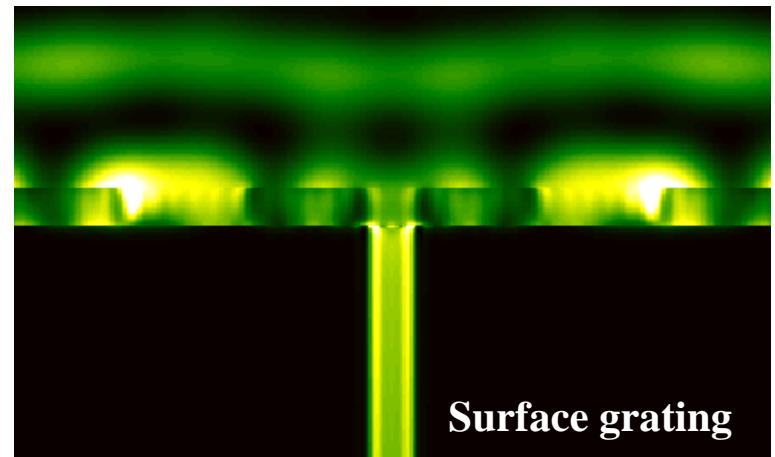
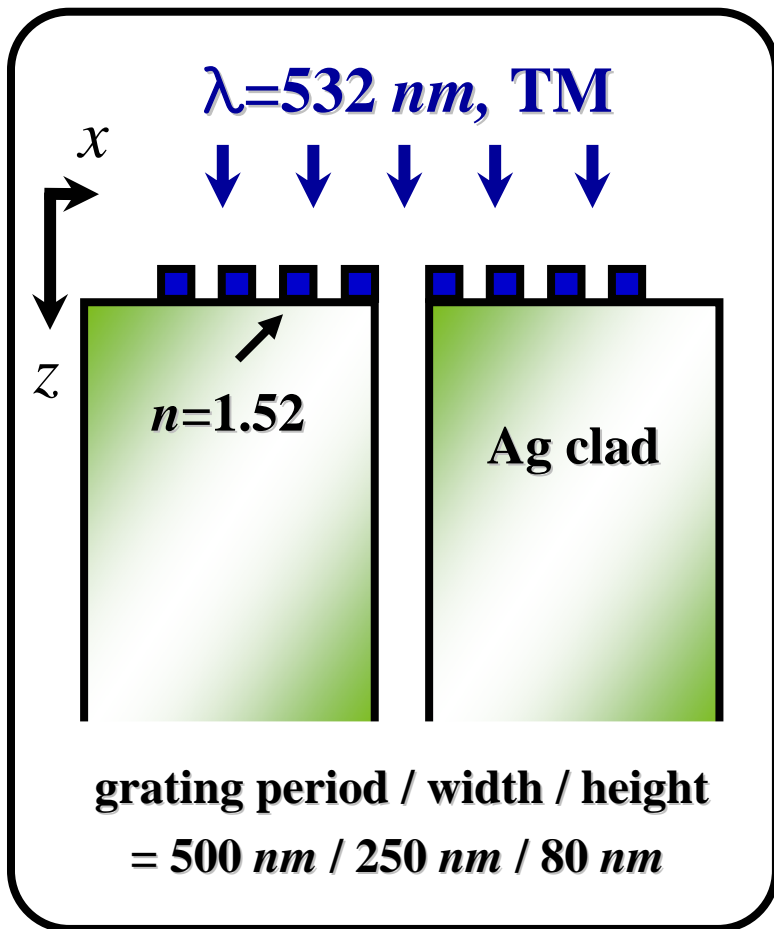
Metal-gap waveguide analysis

Metal-gap waveguide with bottom surface grating

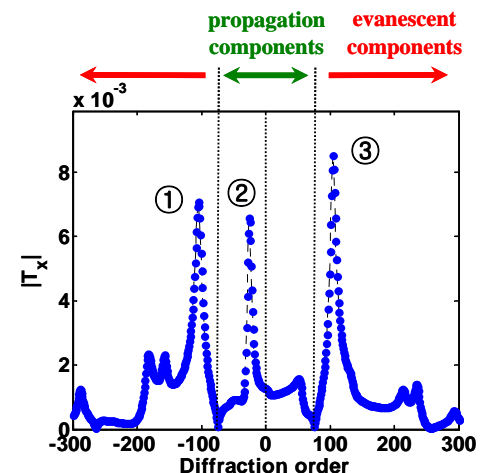
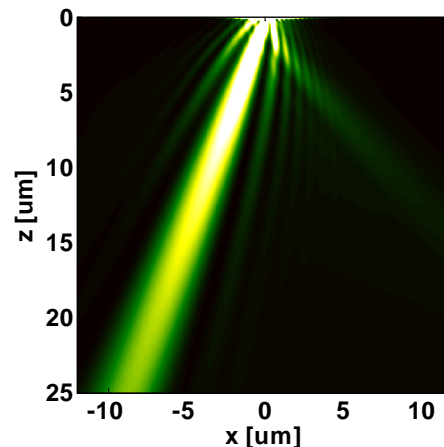
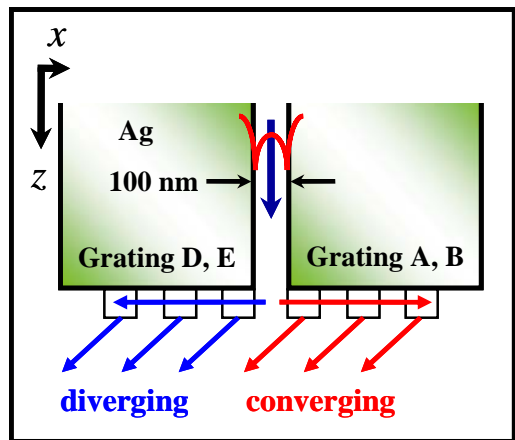
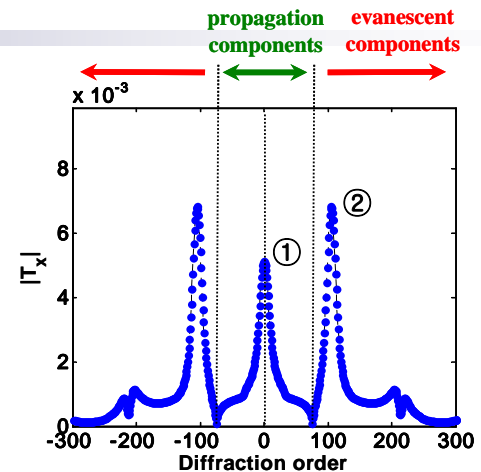
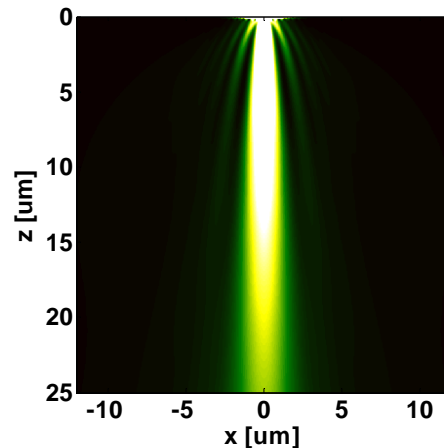
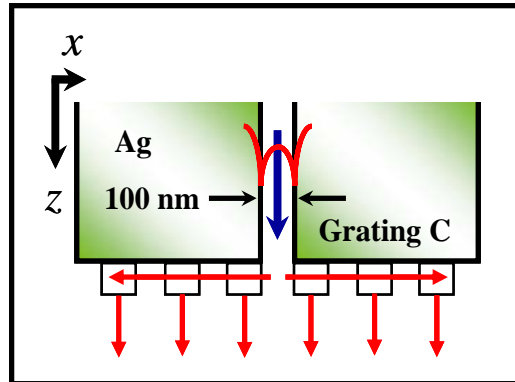


Metal-gap waveguide analysis

- Metal-gap waveguide with upper surface grating



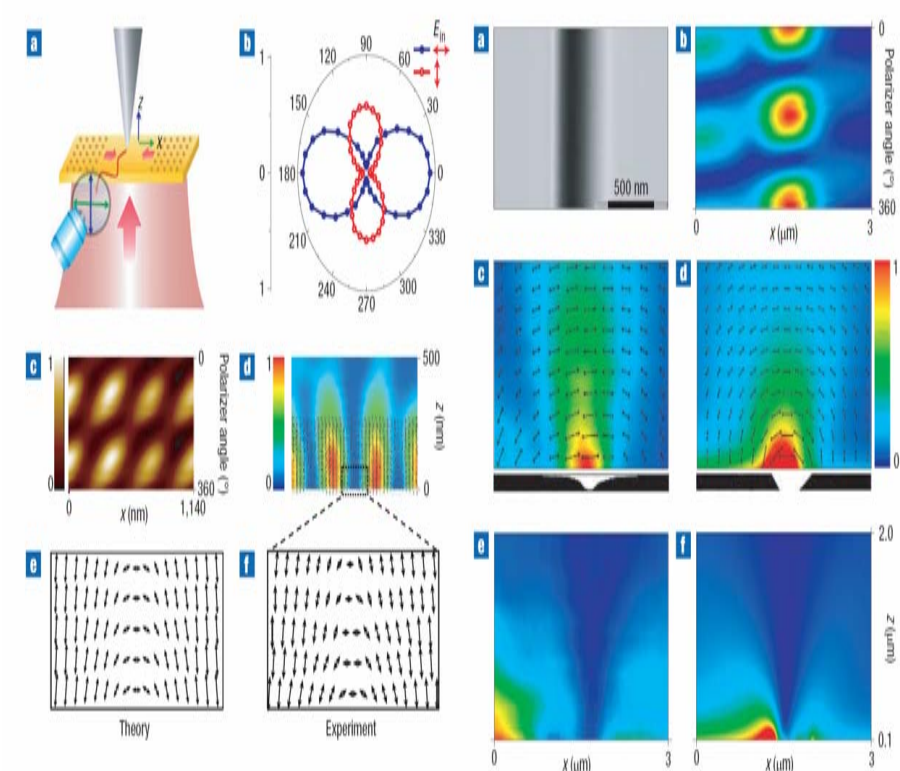
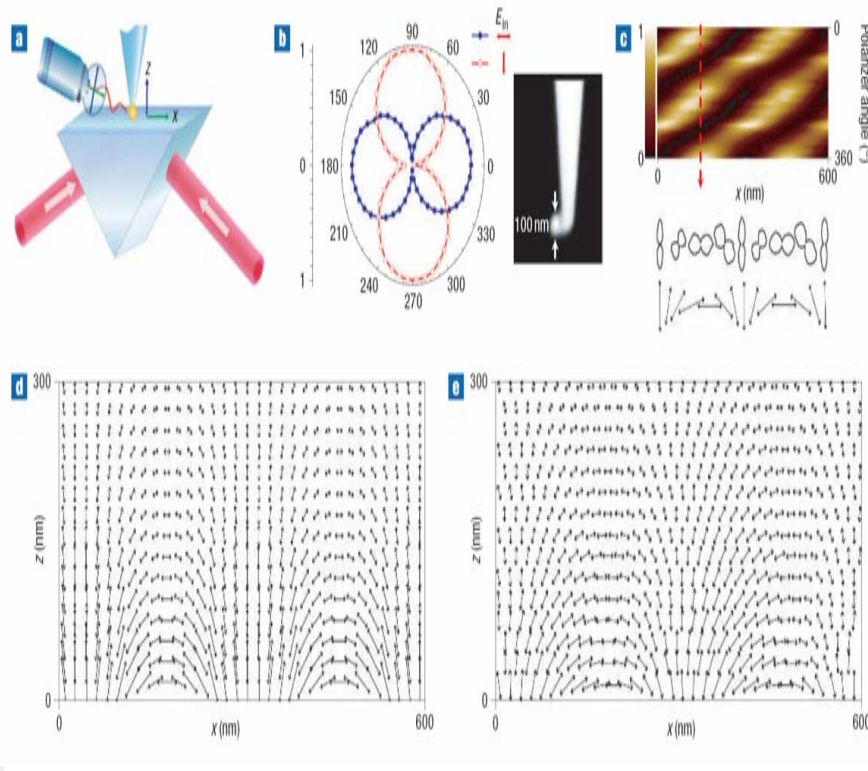
Off-axis directional beaming (*Applied Physics Letters*)



S. Kim, H. Kim, Y. Lim, and B. Lee, “Off-axis directional beaming of optical field diffracted by a single subwavelength metal slit with asymmetric dielectric surface gratings,” *Applied Physics Letters*, vol. 90, no. 5, 051113, 2007.



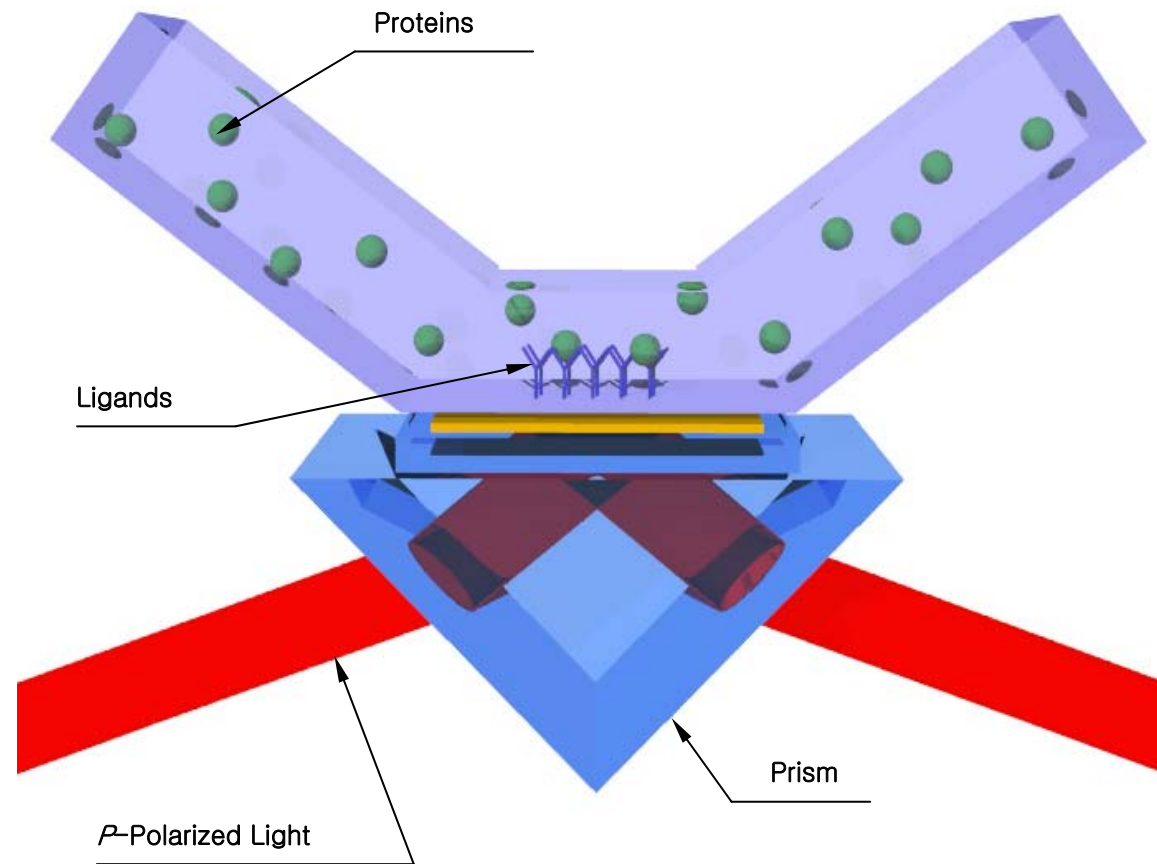
Vector field microscopic imaging of light (*Nature Photonics*)



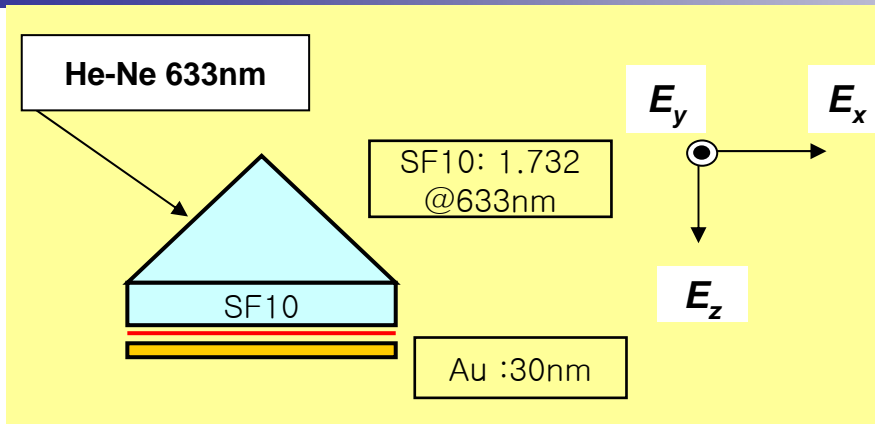
K. G. Lee, H. W. Kihm, J. E. Kihm, W. J. Choi, H. Kim, C. Ropers, D. J. Park, Y. C. Yoon, S. B. Choi, D. H. Woo, J. Kim, B. Lee, Q. H. Park, C. Lienau, and D. S. Kim, "Vector field microscopic imaging of light," *Nature Photonics*, vol. 1, no. 1, pp. 53-56, 2007.



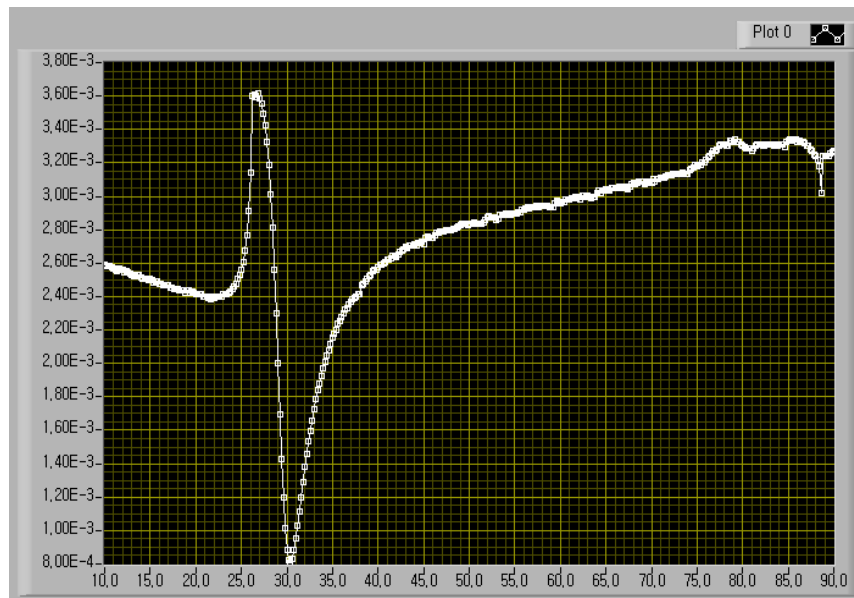
SPR biosensors



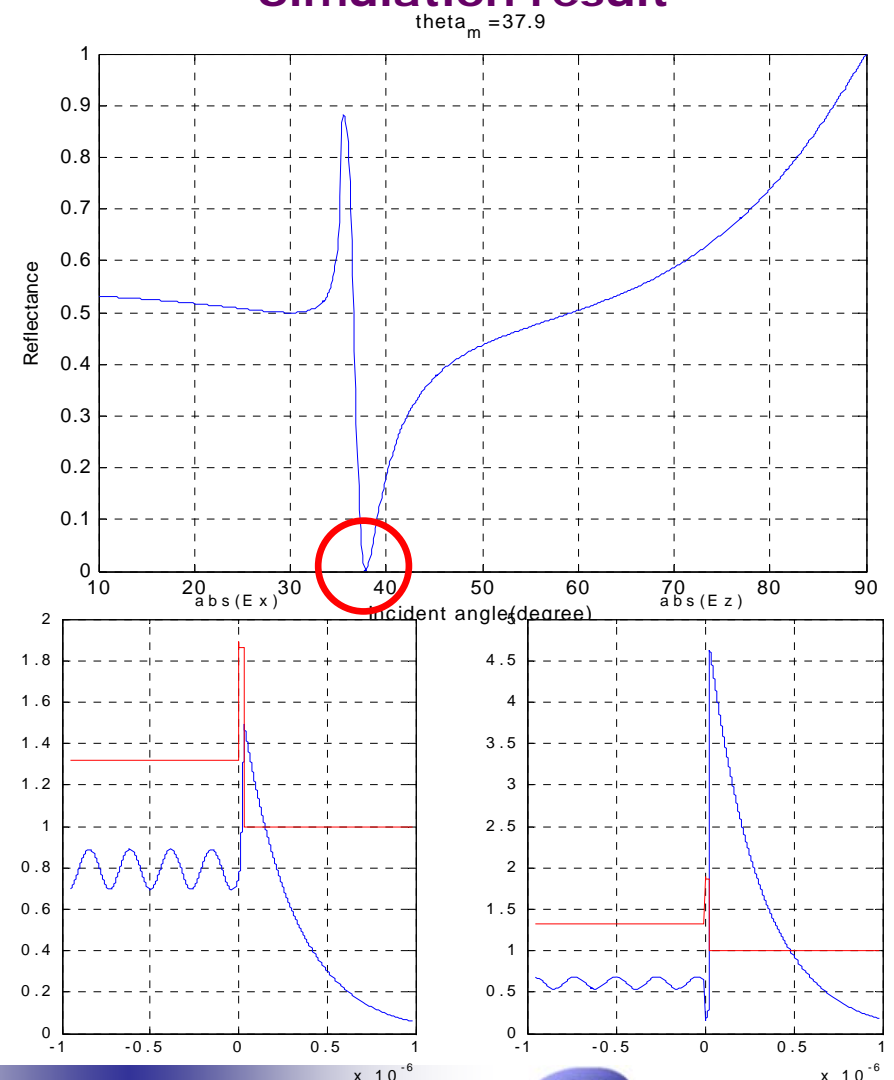
Surface plasmon resonance on a flat boundary



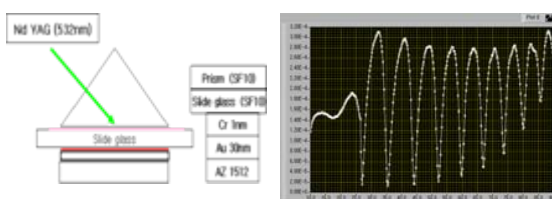
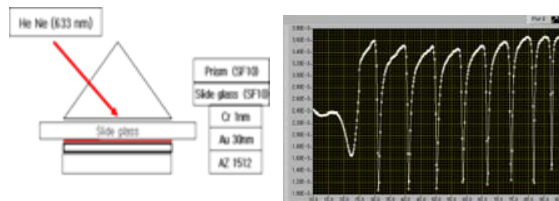
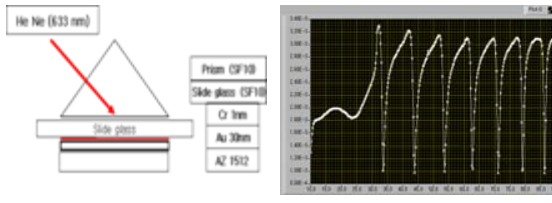
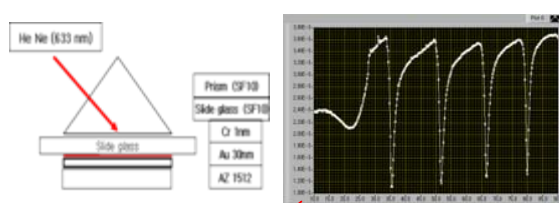
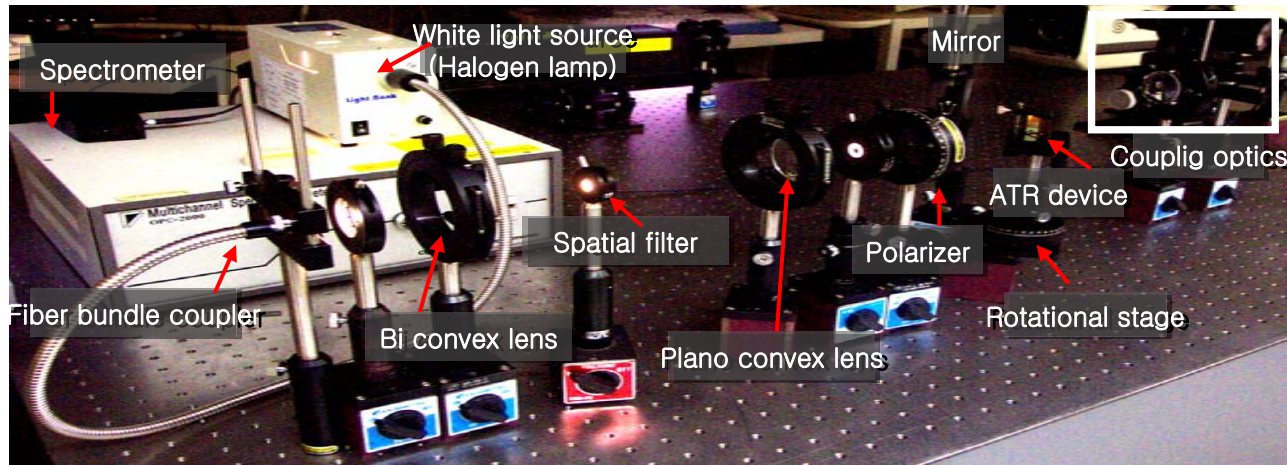
Experimental result



Simulation result



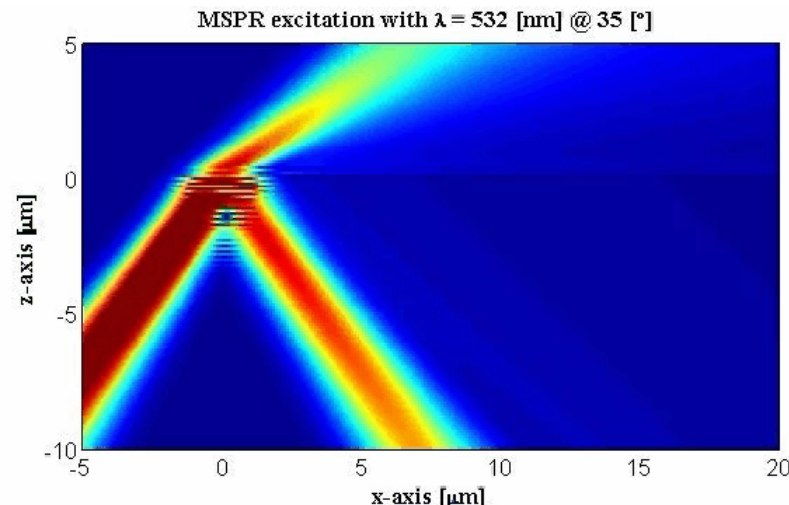
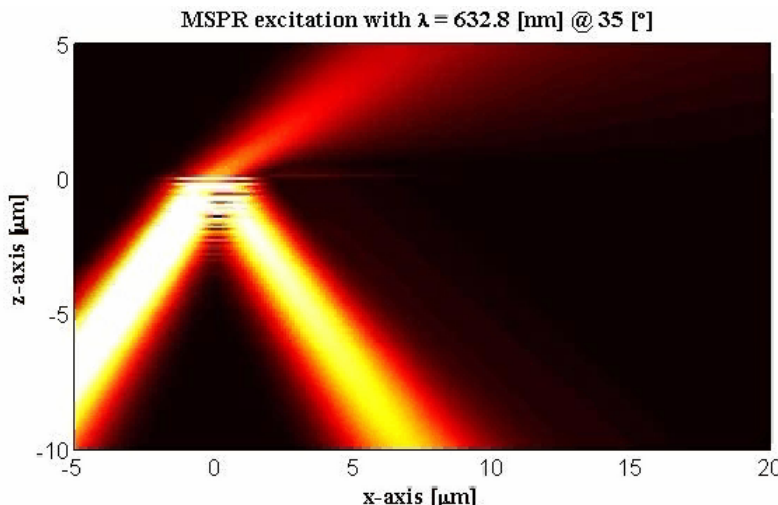
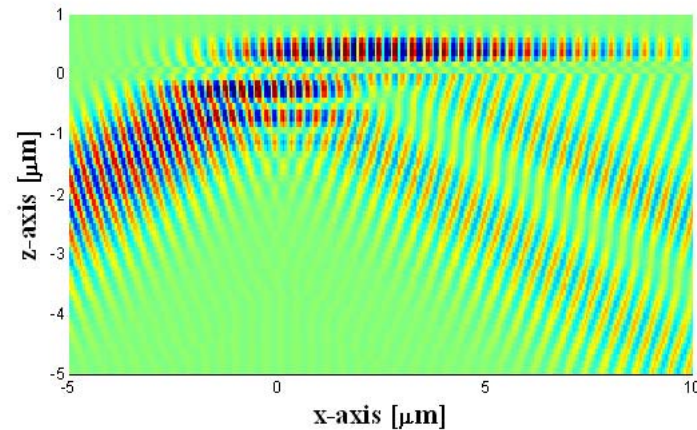
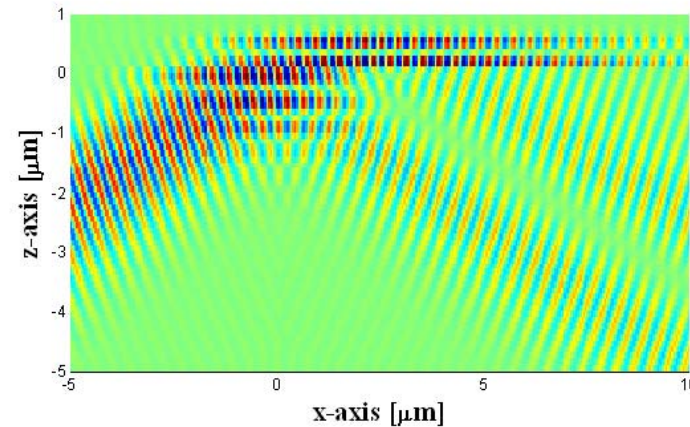
Multiple SPR on multilayer structures



SPR analysis

K. Choi, H. Kim, Y. Lim, S. Kim, and B. Lee, *Optics Express*, vol. 13, no. 22, pp. 8866-8874, 2005.

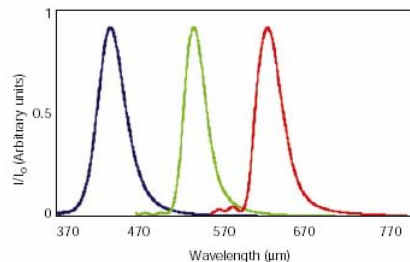
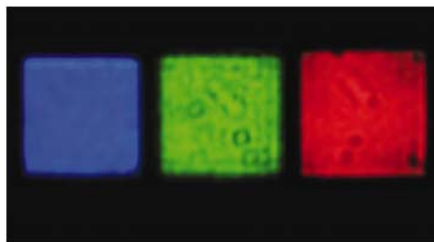
Visualization of SPR using R-TMM and Gaussian angular spectrum decomposition



Surface plasmon applications

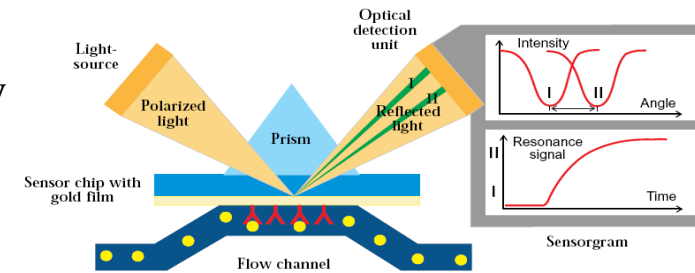
SPP Applications

- Surface sensitive techniques, SPR microscopy
- SPR technologies and a wide range of photonic ICs.

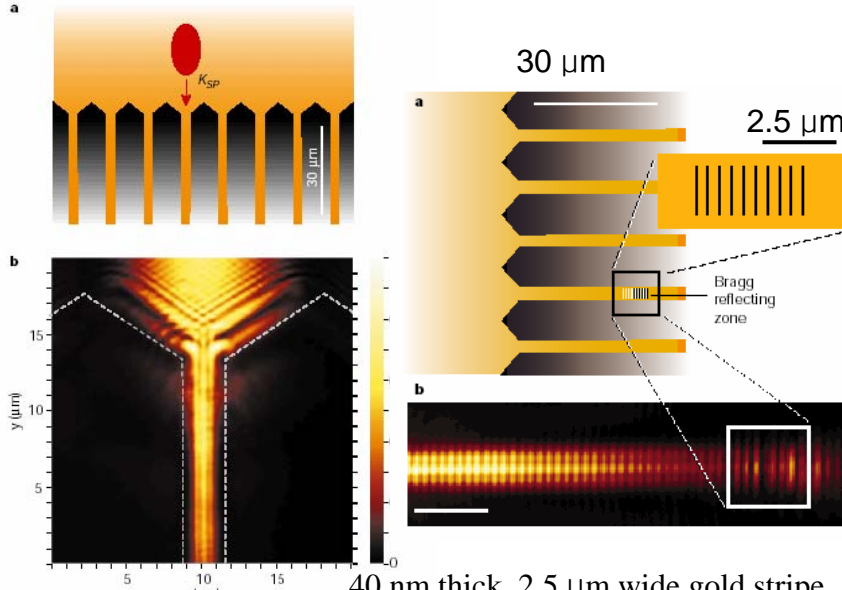


Ag Film with hole arrays
(Period = 300, 450, 550nm
Hole diameter=155,180,225nm)

A. Degiron et al. *Appl. Phys. Lett.* **81**, 4327 (2002).



Waveguides of surface plasmons
Surface plasmon Bragg reflectors
Bio- and flow-sensors using SPR
Light transmission enhancement
Laser beam shaping



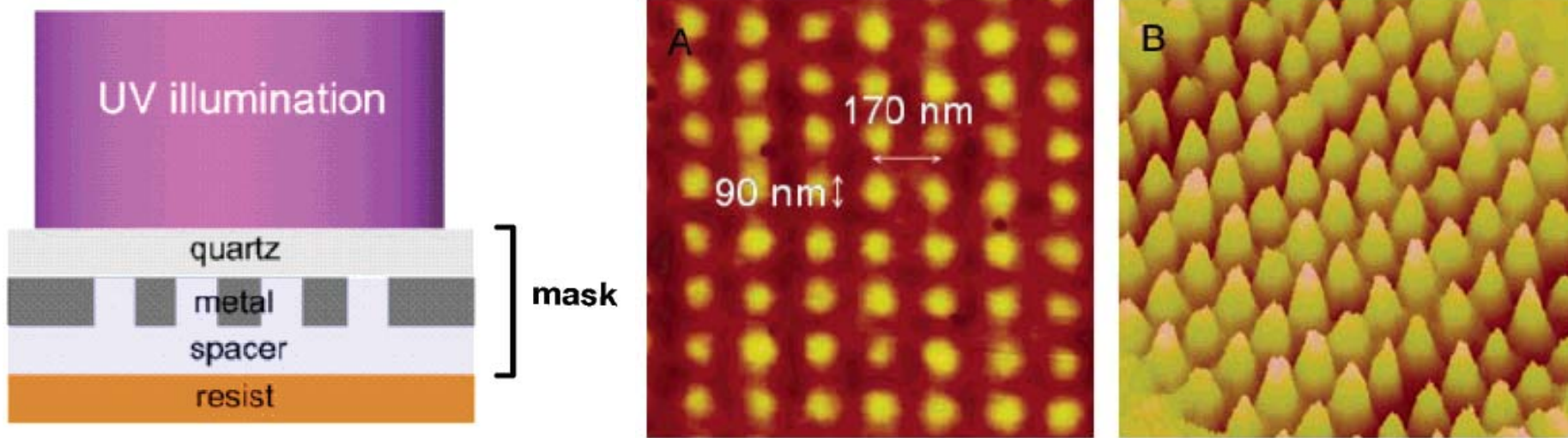
40 nm thick, 2.5 μm wide gold stripe lying on a glass substrate

J. C. Weeber et al., *Phys. Rev. B* **64**, 045411(2001).



Plasmonic nanolithography

W. Srituravanich, N. Fang, C. Sun, Q. Luo, and X. Zhang,
Nano Letters, vol . 4, no. 6, pp. 1085-1088, 2004.



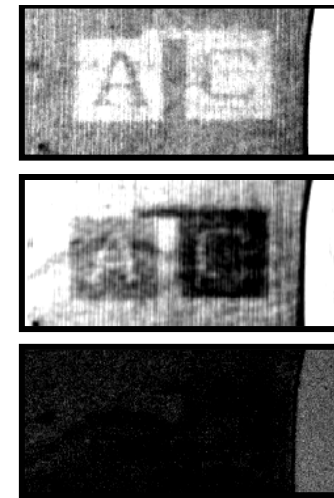
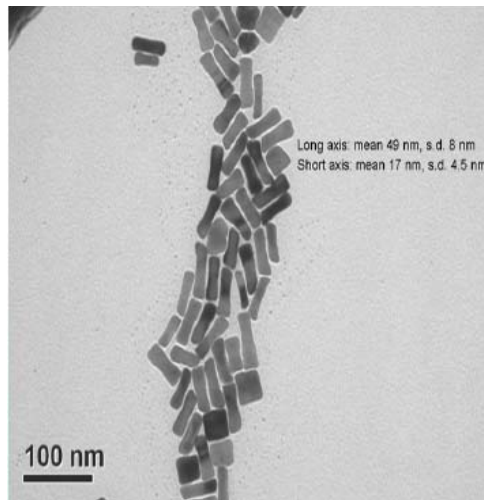
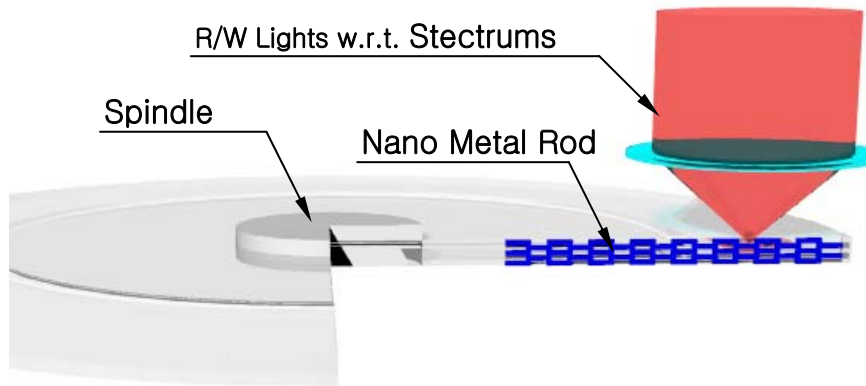
Metal mask : 90nm holes, 170nm period

Surface plasmons

1. Much shorter wavelength compared to the excitation light wavelength
2. E-field intensity of surface plasmons can be boosted by several orders of magnitude compared to the excitation light



Nano metal rod memory



Reading at
760nm
690nm
950nm

Swinburne University
of Technology

Resonant surface plasmon couplings (SuperLens)

Superlens-based nanopatterning

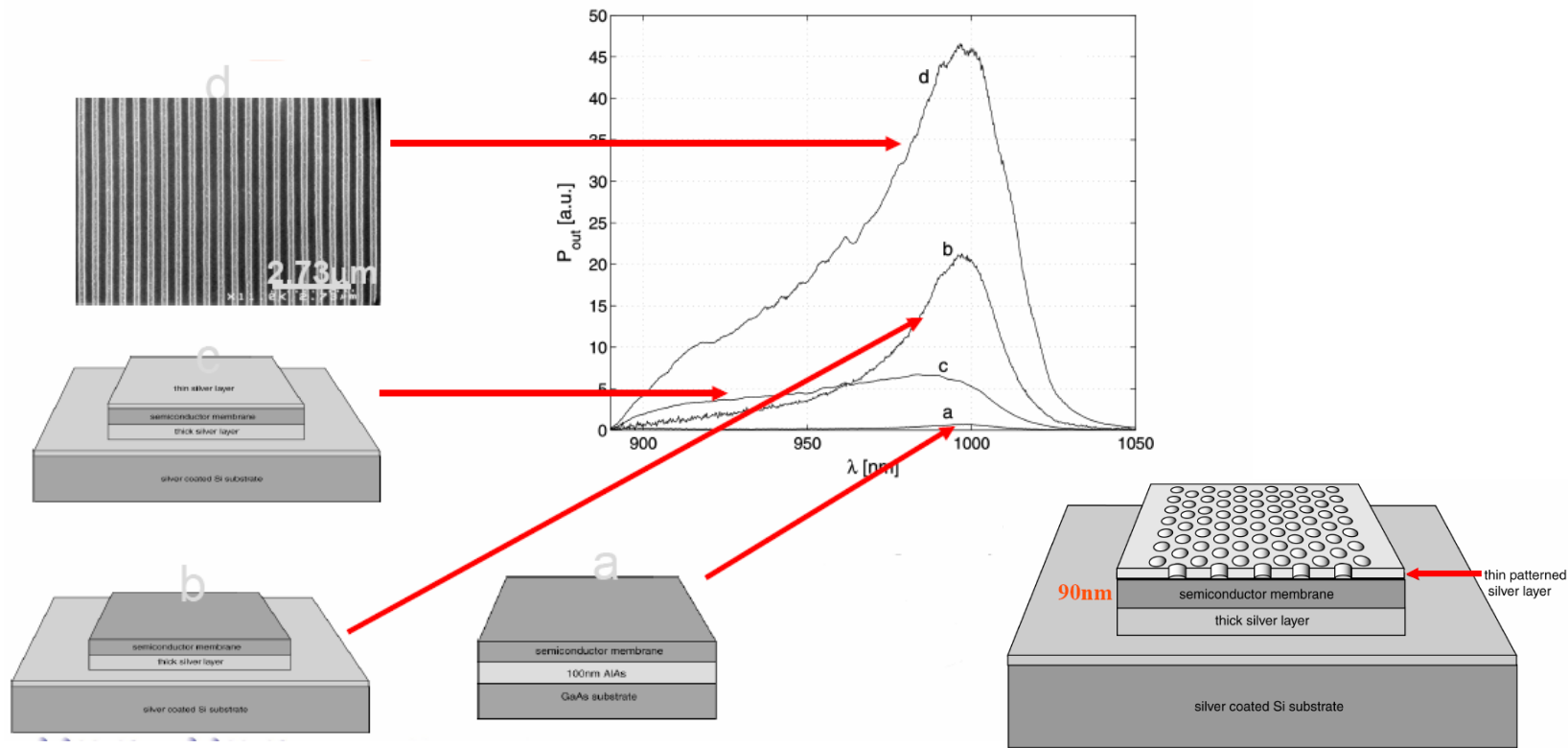
- A flat plane of NRM behaves as superlens and amplifies evanescent waves in near-field through a series of plasmon resonances.
- This allows super-resolutions below diffraction limit.
- Experimentally achieved improvements in UV range: 5-10x beyond the operating wavelength
- Applicable for direct imaging of evanescent modes, thus for immediate recognition of analytes
- Also applicable for nanopatterning through subwavelength contact lithography



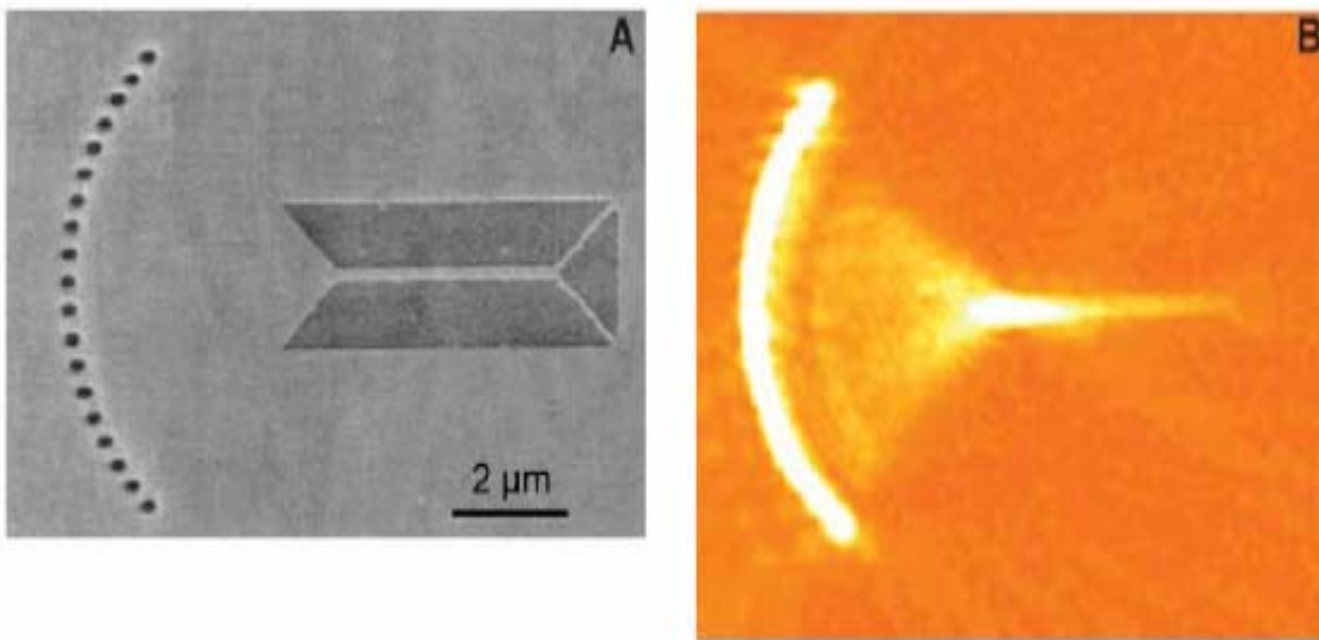
Resonant surface plasmon couplings (LED)

Ultrahigh efficiency LED via plasmon light extraction

46x PL enhancement for wafers with periodicities of 480nm and 650nm.



Nanodot focusing array

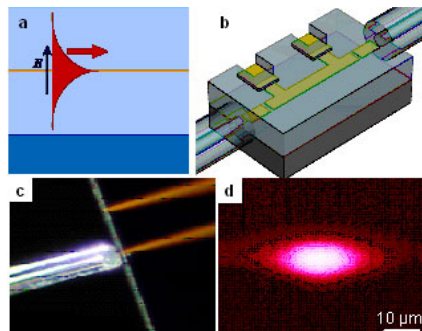


- (A) SEM image of a nanodot focusing array coupled to a 250-nm-wide Ag strip guide.
- (B) NSOM image of the SP intensity showing subwavelength focusing.

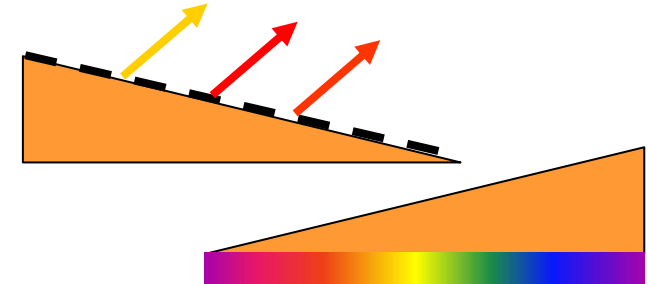
W. Nomura, M. Ohtsu, and T. Yatsui, *Appl. Phys. Lett.* **86**, 181108 (2005).

Plasmonic toolbox: ω , $e(\omega)$, d - engineer $\lambda(\omega)$

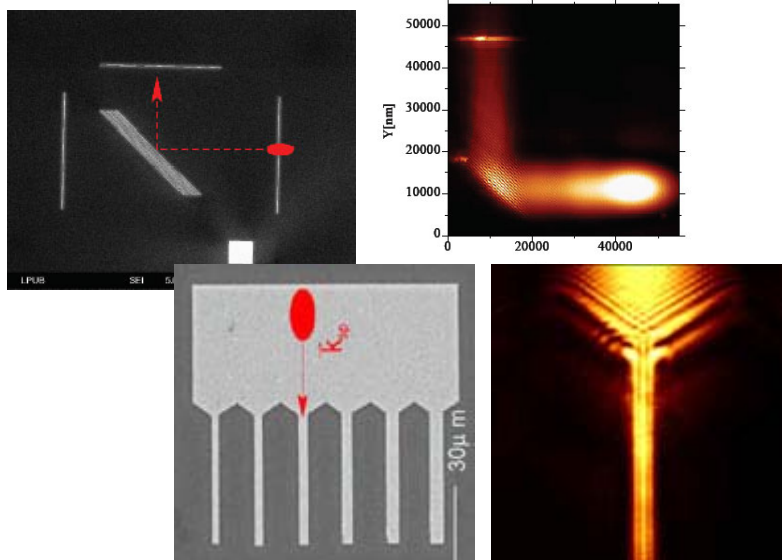
Plasmonic modulator & IC



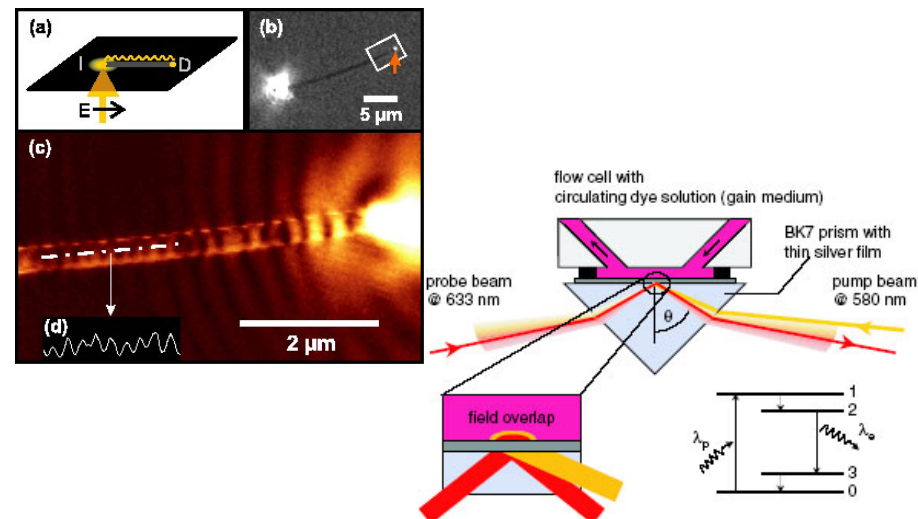
Plasmonic multiplexer & Concentrator



Plasmonic Bragg mirror & waveguide



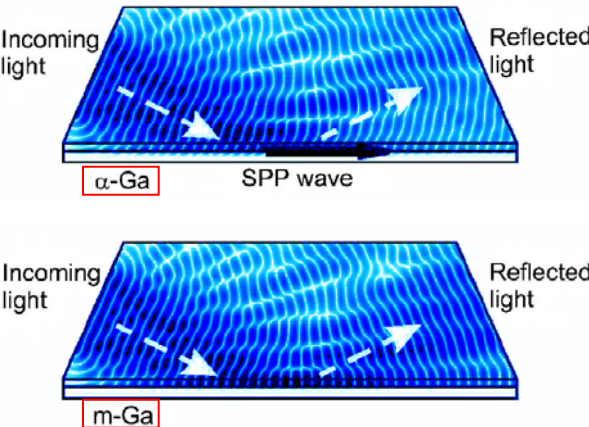
Plasmonic resonator & laser



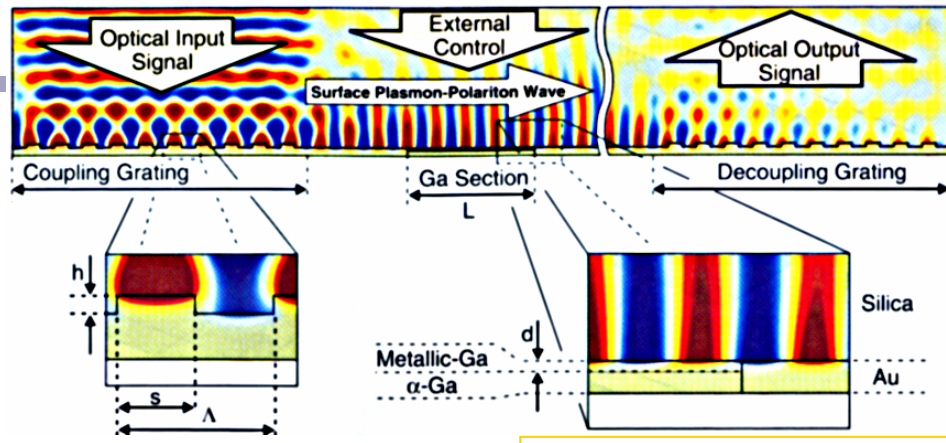
<http://www.plasmonanodevices.org/>

Active plasmonics: Electrical/optical active switching/amplification of SPP

Nanoscale light-induced structural transformation
in the Ga layer

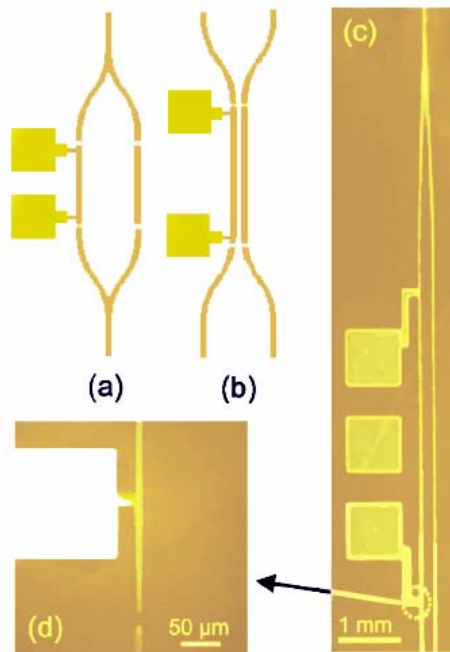
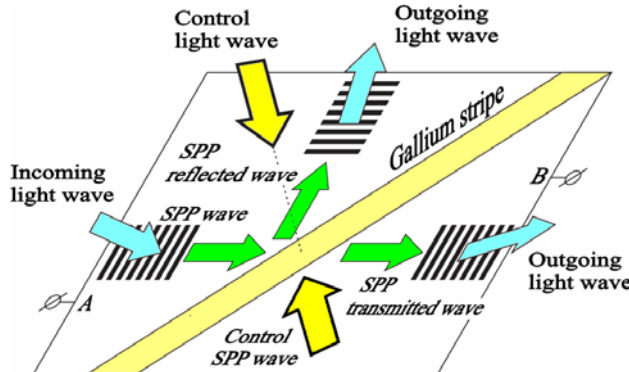


A. V. Krasavin *et al.*,
Appl. Phys. Lett. 85, 3369 (2004).



A. V. Krasavin *et al.*,
Appl. Phys. Lett. 84, 1416 (2003).

Thermo-optical control of the propagation of SPPs
propagating on gold stripe embedded in polymer



• Modulators and switches

T. Nikolajsen *et al.*,
Appl. Phys. Lett. 85, 5833 (2004)



Left-handed material

- V.G. Veselago, Soviet Physics Uspekhi 10, 509 (1968)



$$k \sin \phi = k_1 \sin \phi_1.$$

Однако последнее равенство удовлетворяется как при угле ϕ_1 , так и при угле $\pi - \phi_1$.

Требуя по-прежнему, чтобы энергия во второй среде *оттекала* от границы раздела, мы приходим тогда к тому, что фаза должна набегать на эту границу и, следовательно, направление распространения преломленной волны будет составлять с нормалью угол

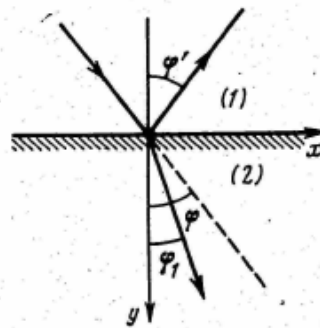


Рис. 12

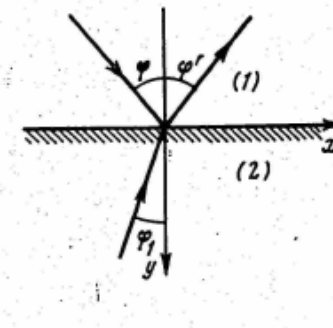


Рис. 13

$\pi - \phi_1$. Как ни непривычно такое построение, но, конечно, ничего удивительного в нем нет, ибо фазовая скорость еще ничего не говорит о направлении потока энергии.

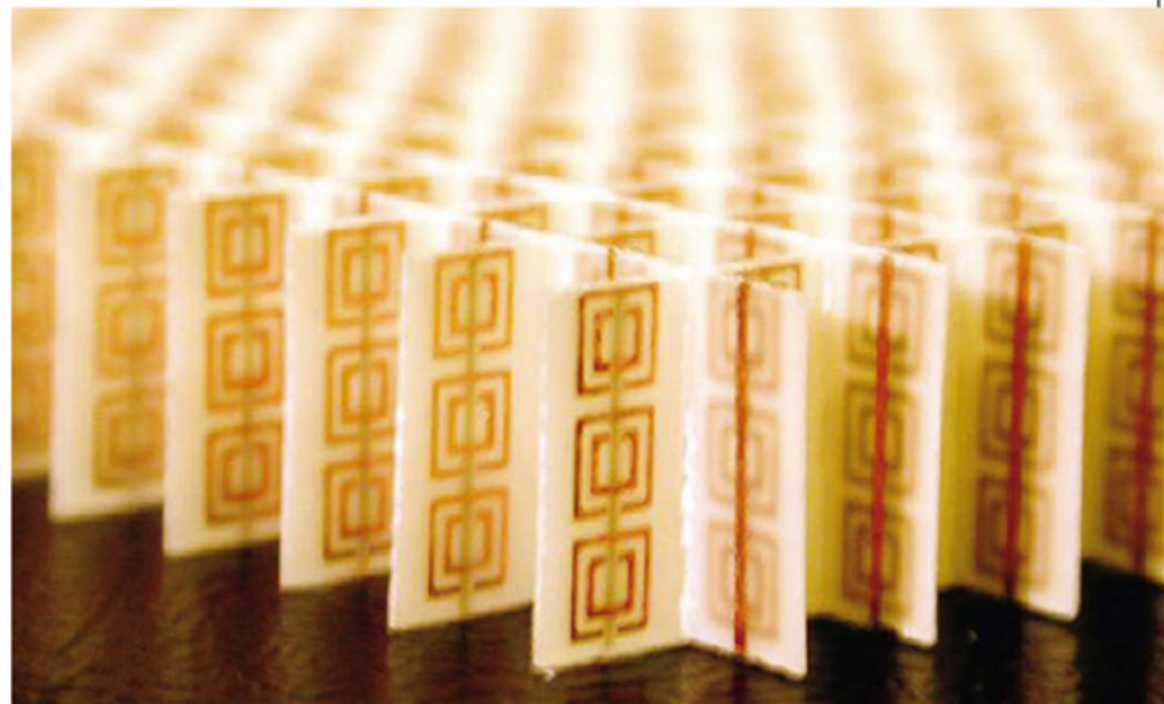
A lens less ordinary

In the 1960s, a Russian physicist considered the properties of a material that didn't yet exist. Now researchers appear to have fulfilled his predictions — but is everything as it seems? Liesbeth Venema investigates.

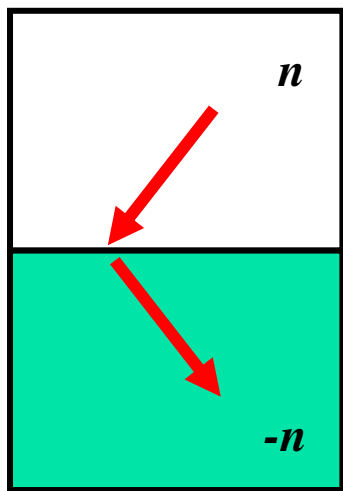
There are some truths in physics on which we have come to depend. Light rays, for example, bend when they cross the boundary between two materials. That's why an oar dipped into water appears to bend towards the surface, and why the pool itself looks shallower than it really is.

But this familiar phenomenon, called refraction, is beginning to look less straightforward. In the lab of David Smith, a physicist at the University of California, San Diego, a strange array of metal wires and loops has been pieced together. In April 2001, Smith and his team showed that this construction, which they refer to as a 'metamaterial', has a peculiar property: it bends electromagnetic waves in the opposite direction to normal materials¹.

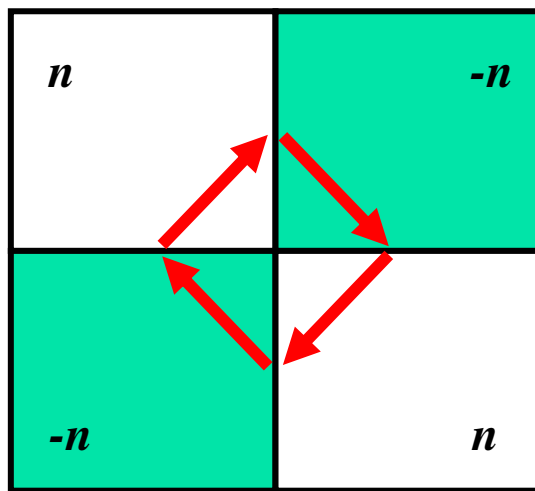
If a pool of water had this property, known as negative refraction, oars would bend away from the surface, and the pool



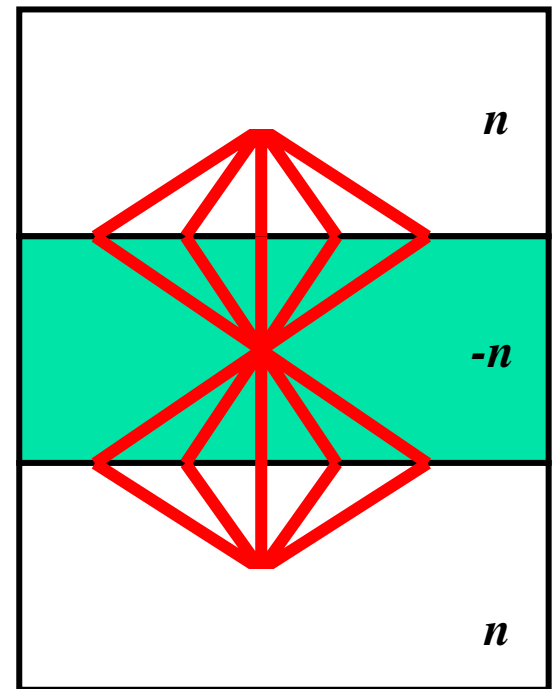
Light propagation in negative index material



Negative refraction



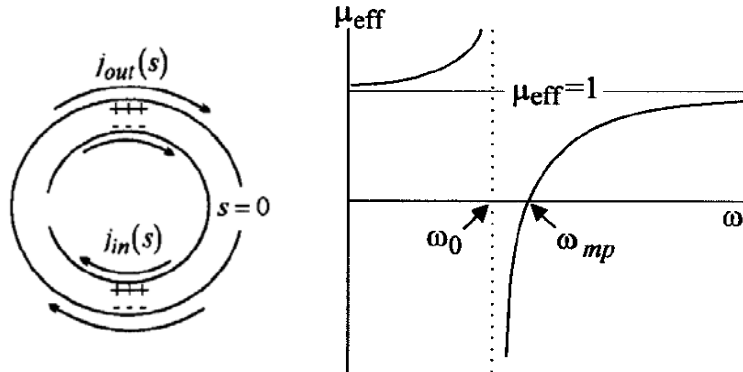
**Formation of
an open cavity**



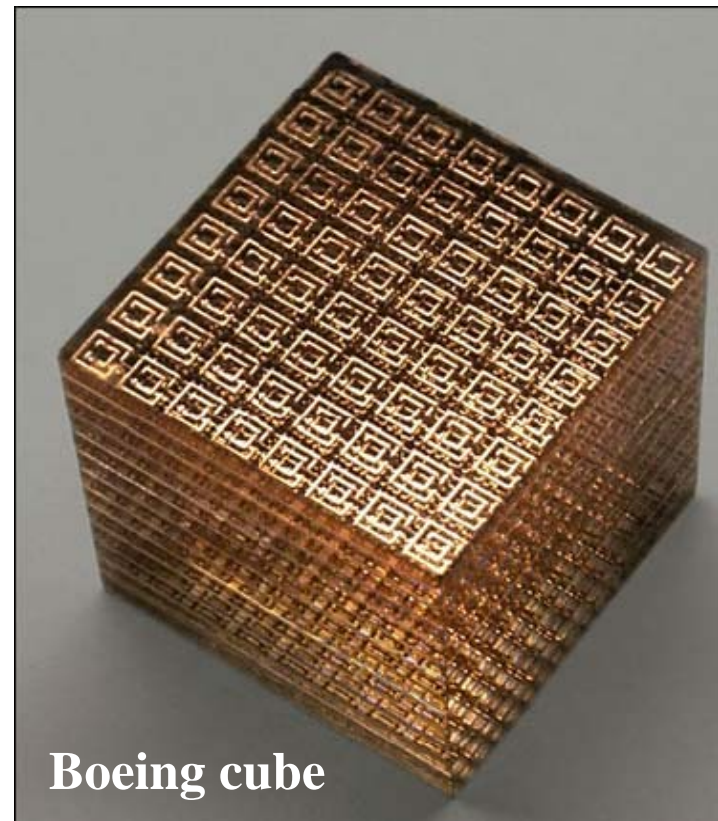
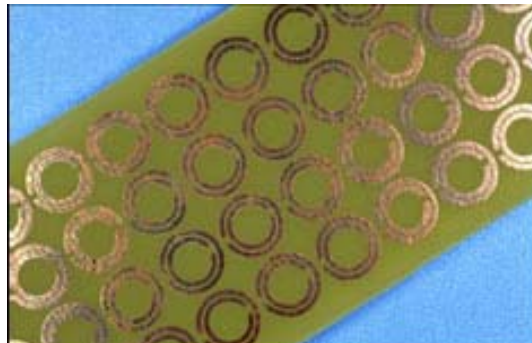
Imaging by a slab

Split ring resonators

- J.B. Pendry et al., IEEE transactions on microwave theory and techniques 47, 2075 (1999).



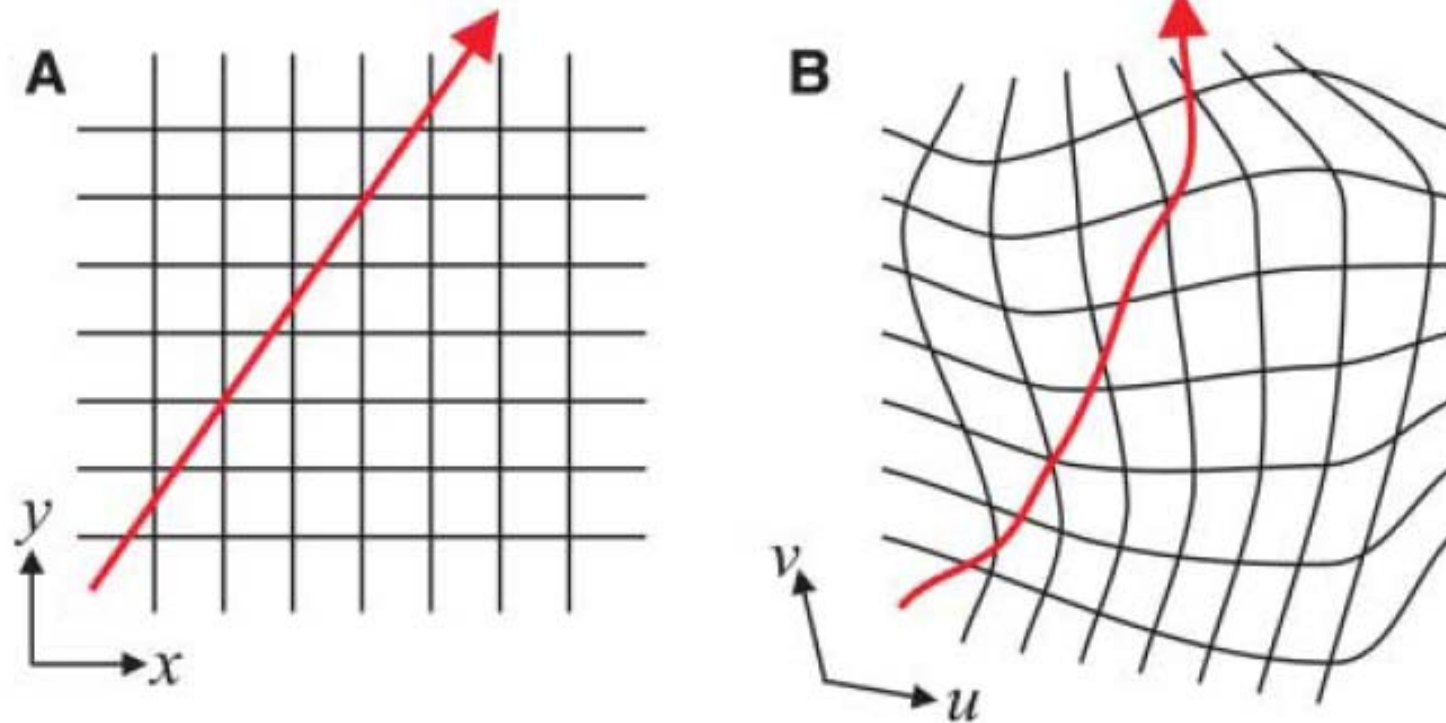
Effective magnetic permeability



Boeing cube

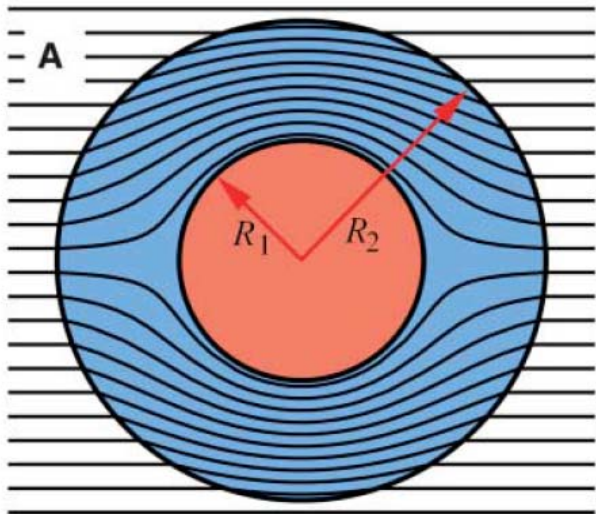
Coordinate transform

- G.R. Newkome et al., Science 312, 1782 (2006).



When the coordinate is transformed, the Maxwell equations have exactly the same form but the ϵ and μ are scaled by a common factor.

Basic concept of cloaking



Any radiation attempting to penetrate the secure volume is smoothly guided around by the cloak to emerge traveling in the same direction as if it had passed through the empty volume of space.

region $r < R_2$ → **region $R_1 < r < R_2$**

$$r' = R_1 + r(R_2 - R_1) / R_2$$

$$\theta' = \theta$$

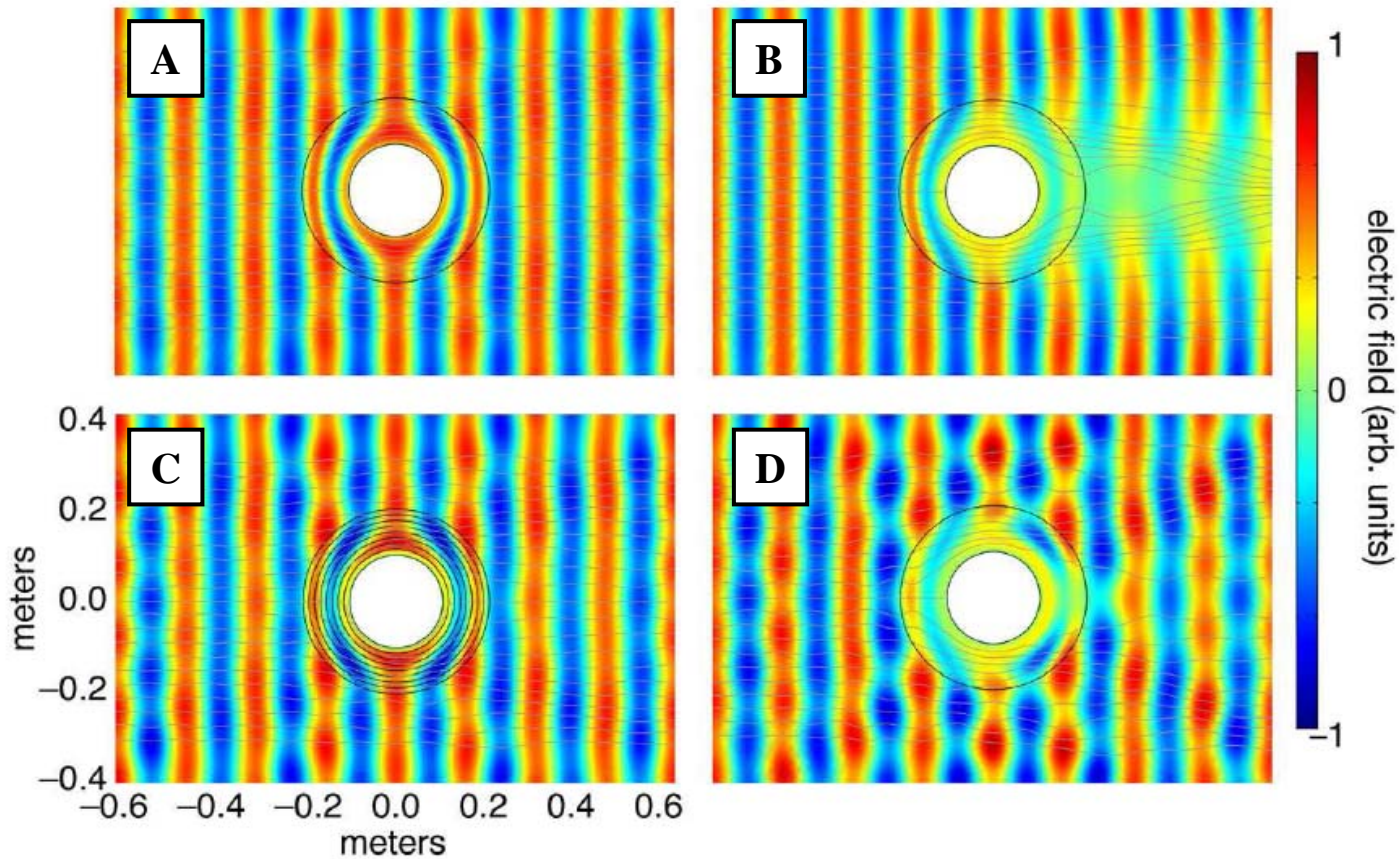
$$\phi' = \phi$$

$$\varepsilon'_{r'} = \mu'_{r'} = \frac{R_2}{R_2 - R_1} \frac{(r' - R_1)^2}{r'}$$

$$\varepsilon'_{\theta'} = \mu'_{\theta'} = \frac{R_2}{R_2 - R_1}$$

$$\varepsilon'_{\phi'} = \mu'_{\phi'} = \frac{R_2}{R_2 - R_1}$$

Simulation of cloaking structures



A : Ideal parameter & lossless

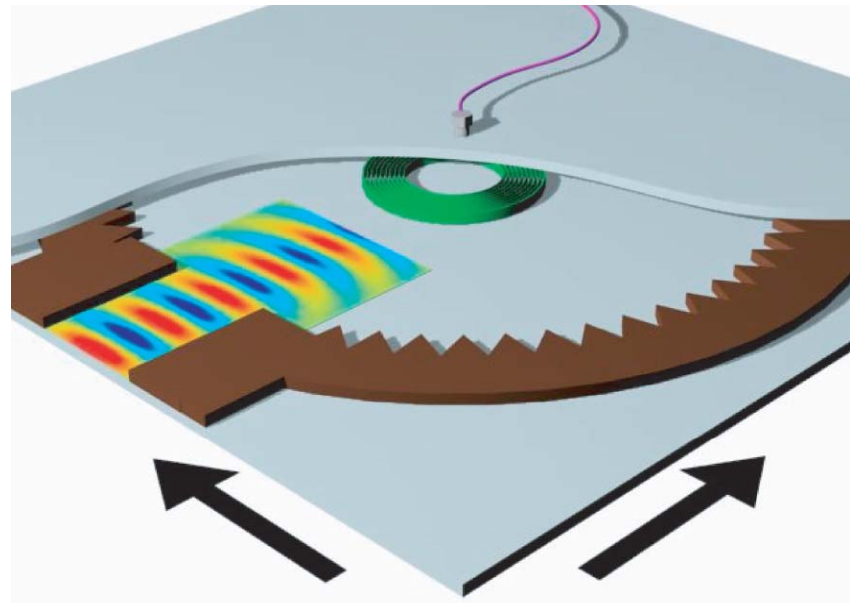
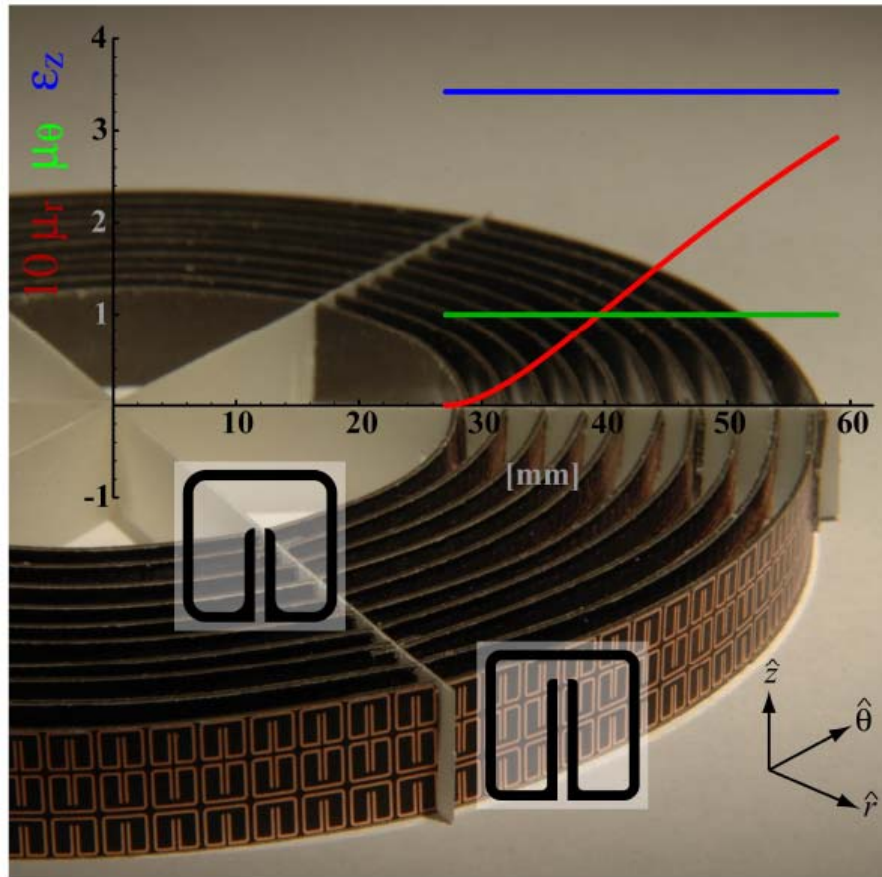
C : 8-layers approximation

B : Ideal parameter & lossy

D : Reduced approximation

Microwave cloaking structure

- D. Schurig et al., Science, in press (2006).



레이저가 늦게 발명된 이유



Charles H. Townes (1915-)

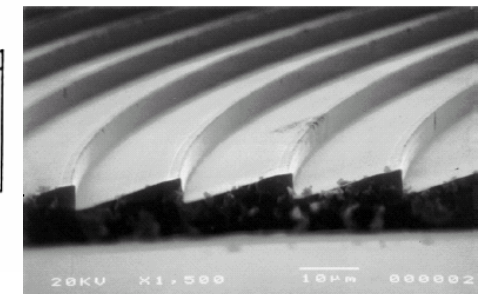
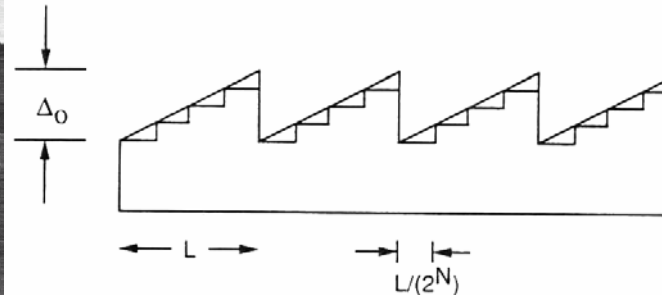
“대부분의 물리학자들은 전자공학과 증폭기에 대해서 몰랐었고, 전기공학자들은 대개 양자역학을 배우지 않았다. 하지만 제 2차 세계대전으로 인해 레이다 (radar) 개발을 위해 공학자들과 자연과학자들이 함께 일하게 되었고, 물리학자들이 전자공학에 접근할 수 있게 되었다.”

(*IEEE J. Selected Topics in Quantum Electronics*, Nov./Dec. issue, 2000)

Lord Rayleigh



Never say ‘Never’!



“...If it were possible to introduce at every part of the aperture of the grating an arbitrary retardation, all the light might be concentrated in any desired spectrum. By supposing the retardation to vary uniformly and continuously we fall upon the case of an ordinary prism; but there is then no diffraction spectrum in the usual sense. To obtain such it would be necessary that the retardation should gradually alter by a wave-length in passing over any element of the grating, and then fall back to its previous value, thus springing suddenly over a wave-length. It is not likely that such a result will ever be fully attained in practice; but the case is worth stating, in order to show that there is no theoretical limit to the concentration of light of assigned wave-length in one spectrum...”

Encyclopaedia Britannica, 9th ed., Vol. 24, “Wave Theory of Light” (New York, Charles Schribner’s Sons, 1888), p. 437